Energies **2012**, *5*, 1782-1815; doi:10.3390/en5061782

OPEN ACCESS

energies

ISSN 1996-1073

www.mdpi.com/journal/energies

Article

Dynamic Output Feedback Power-Level Control for the MHTGR Based On Iterative Damping Assignment

Zhe Dong

Institute of Nuclear and New Energy Technology, Tsinghua University, Beijing 100084, China; E-Mail: dongzhe@mail.tsinghua.edu.cn; Tel.: +86-10-6279-6425

Received: 26 April 2012; in revised form: 5 June 2012 / Accepted: 7 June 2012 / Published: 13 June 2012

Abstract: Because of its strong inherent safety features and high outlet temperature, the modular high temperature gas-cooled nuclear reactor (MHTGR) is already seen as the central part of the next generation of nuclear plants. Such power plants are being considered for industrial applications with a wide range of power levels, and thus power-level control is an important technique for their efficient and stable operation. Stimulated by the high regulation performance provided by nonlinear controllers, a novel dynamic output-feedback nonlinear power-level regulator is developed in this paper based on the technique of iterative damping assignment (IDA). This control strategy can provide the L_2 disturbance attenuation performance under modeling uncertainty or exterior disturbance, and can also guarantee the globally asymptotic closed-loop stability without uncertainty and disturbance. This newly built control strategy is then applied to the power-level regulation of the HTR-PM plant, and numerical simulation results show both the feasibility and high performance of this newly-built control strategy. Furthermore, the relationship between the values of the parameters and the performance of this controller is not only illustrated numerically but also analyzed theoretically.

Keywords: modular high temperature gas-cooled reactor (MHTGR); power-level control; iteratively damping assignment; L_2 disturbance attenuation

1. Introduction

After the severe nuclear accident at Fukushima, the safety issues of nuclear reactors have become much more significant than before. Because of its inherent safety characteristic and economic competitive power, the modular high-temperature gas-cooled reactor (MHTGR) is seen as the central

part of the next generation nuclear plant (NGNP). MHTGRs use helium as coolant and graphite as both moderator and structural material, and its fuel elements contain thousands of very small coated particles that are embedded in a graphite matrix. The coatings surrounding the particle kernel produce a robust fuel form by acting as the containment boundary for radioactive material. The crucial inherent safety feature is guaranteed by the low power density and the slim shape of the reactor core [1–3], which makes the MHTGR meet and exceed current nuclear standards in reliability, waste management and safety. Moreover, the MHTGR can provide heat for industrial process at temperatures from 700 to 950 °C, which opens a door for a wider range of commercial applications than that of current light water reactors operating near 300 °C. Study on the MHTGR technology began in China at the end of the 1970s. A 10 MW_{th} pebble-bed high temperature gas-cooled test reactor (HTR-10), which was built at Institute of Nuclear and New Energy Technology (INET) of Tsinghua University [4], achieved its criticality in December 2000 and full power level in January 2003. Six safety demonstration tests have also been done on the HTR-10, which have manifested both the inherent safety feature and the self-stabilizing features [5].

Figure 1. Schematic structure of the HTR-PM power plant.

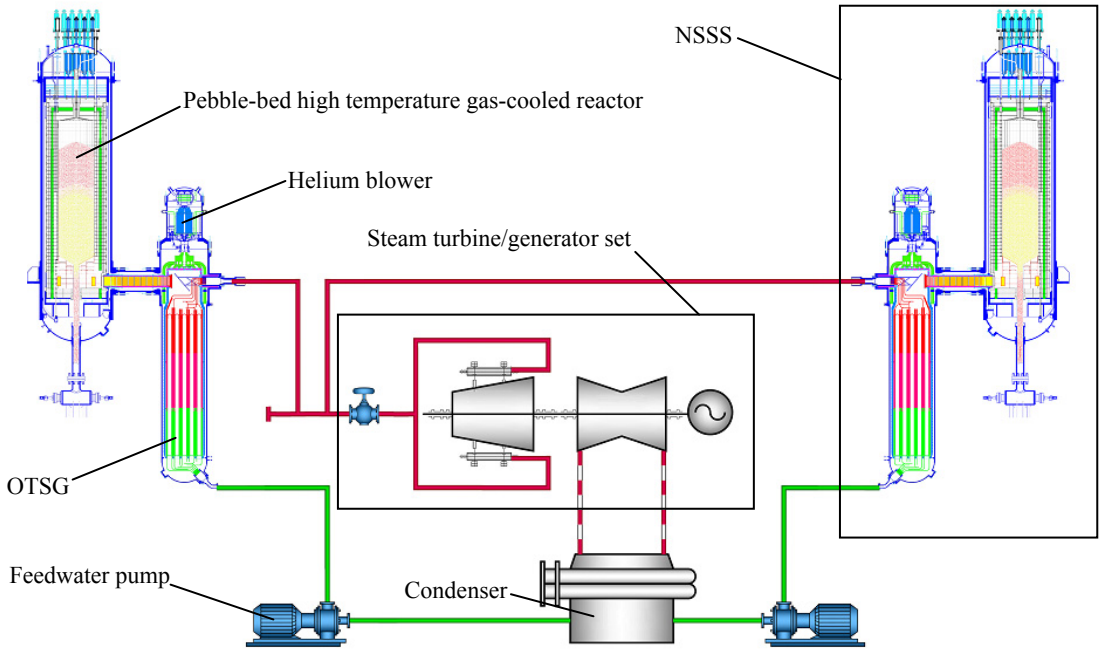

Based upon the HTR-10, a high temperature gas-cooled reactor pebble-bed module (HTR-PM) project has then been proposed [6,7]. The HTR-PM plant consists of two pebble-bed one-zone module reactors of combined 2 × 250 MW_{th} power, and adopts the operation scheme of two modules connected to one steam turbine/generator set. Here, the module is a nuclear steam supplying system (NSSS) composed of an MHTGR, a helical coiled once-through steam generator (OTSG) and some connecting pipes. The MHTGR and OTSG of one NSSS are arranged side by side and housed in independent steel pressure vessels, and the schematic view of the HTR-PM plant is illustrated in Figure 1.

It is exceedingly clear that safe, stable and efficient operation is a key requirement for the various industrial applications of the MHTGR power plants such as electricity production, process heat sources, *etc*. Power-level regulation is just one of the most significant techniques guaranteeing economic and stable control performance and is very meaningful for the operation of the MHTGR. The basic principle of the power-level control is generating the insertion and withdrawal speed signal of the control rods to regulate the plant power according to a demand signal based upon the measurement of the neutron concentration, coolant temperature, control rod positions, *etc*. Though the classical output feedback power-level control still dominates commercial nuclear power plant operation, due to the development of the current high speed industrial microprocessors, it is possible now to implement more modern control strategies for improving regulation performance, which has led to the development of a series of promising power-level controllers during the past two decades. Combining the features of both the static output feedback and the state feedback, Edwards *et al.* [8] developed the state feedback assisted classical controller (SFAC) which utilizes the state-feedback to modify the demand signal for an embedded classical output feedback controller, and is quite useful for the existing power plant implementation since it leaves the current classical feedback loop in place. In order for strengthening the robustness of the SFAC, the linear quadratic Gaussian regulation with loop transfer recovery (LQG/LTR) technique is then applied under the SFAC configuration [9,10]. Since the SFAC are essentially linear regulators which guarantees closed-loop stability only near the operating point, it is not suitable for those nuclear plants that should tightly follow the demand signal. Therefore, it is necessary to develop a nonlinear power-level controller with load-following ability. One way to design the nonlinear power-level control is based upon the system model. For example, Shtessel [11] designed a nonlinear power-level control strategy composed of a static state feedback sliding mode controller and a sliding mode state-observer for the TOPAZ II space nuclear reactor. The other way is to use the soft-computing methods such as the artificial neural network [12], fuzzy set [13,14] and genetic algorithm [15]. However, the performances of these intelligent controllers are usually determined by their training samples which are very expensive or not possible to be obtained. The theory of nonlinear power-level control of nuclear reactors is still under development, and there is still no mature controller design approach.

Generalized Hamiltonian system (GHS) theory is a promising control design method for nonlinear systems, whose basic idea is adding dissipative terms to a given dynamic system through feedback in order for the asymptotic closed-loop stability [16]. Both the energy shaping (ES) [17] and the interconnection and damping assignment passivity based control (IDA-PBC) [18] are effective GHS approaches which have been already applied to those mechanical [19], electromechanical [20] and power systems [21–23]. However, these two methods usually result in solving a set of complicated partial differential equations, which limits their application to the complex process systems such as the nuclear reactors. Stimulated by this and the need of designing nonlinear power-level regulation strategy for the MHT-GRs, a novel dynamic output-feedback power-level controller based on iterative damping assignment (IDA-PLC) is presented for the MHTGRs in this paper. The IDA-PLC is composed of a nonlinear state-feedback power-level regulator and a state observer. The regulator is realized by adding damping terms iteratively through state-feedback, and the observer just adopts the well-built dissipation based high-gain filter (DHGF) [24,25]. The IDA-PLC is an L_2 disturbance attenuator when there exist exterior disturbances or modeling uncertainties, and it guarantees the

globally asymptotic closed-loop stability if there is no disturbance and uncertainty. The IDA-PLC is then applied to the power-level control of the NSSS of the HTR-PM plant, and numerical simulation results show not only the feasibility of this newly-built MHTGR power-level control strategy but also the relationship between its performance and its parameters.

The rest part of this paper is organized as follows: both the nonlinear state-space model and the problem formulation are given in Section 2. Section 3 presents the iterative design of the state-feedback power-level regulator. In Section 4, the DHGF is applied to the state-observation of the MHTGR, and the performance of the entire dynamic output-feedback power control strategy formed by both the state feedback regulator and the observer is analyzed theoretically. Simulation results with discussion will be given in Section 5, and some conclusions are drawn in Section 6.

2. Nonlinear State-Space Model and Problem Formulation

2.1. Nonlinear State-Space Model

The dynamic model of the MHTGR can be written as [26,27]:

$$\begin{cases} \dfrac{\mathrm{d}n_\mathrm{r}}{\mathrm{d}t} = \dfrac{\rho_\mathrm{r}-\beta}{\Lambda}n_\mathrm{r} + \dfrac{\beta}{\Lambda}c_\mathrm{r} + \dfrac{n_\mathrm{r}}{\Lambda}\left[\alpha_\mathrm{c}\left(T_\mathrm{c}-T_{\mathrm{c,m}}\right)+\alpha_\mathrm{r}\left(T_\mathrm{r}-T_{\mathrm{r,m}}\right)\right], \\ \dfrac{\mathrm{d}c_\mathrm{r}}{\mathrm{d}t} = \lambda\left(n_\mathrm{r}-c_\mathrm{r}\right), \\ \dfrac{\mathrm{d}T_\mathrm{c}}{\mathrm{d}t} = -\dfrac{\Omega_\mathrm{cd}}{\mu_\mathrm{c}}\left(T_\mathrm{c}-T_\mathrm{d}\right)-\dfrac{\Omega_\mathrm{cr}}{\mu_\mathrm{c}}\left(T_\mathrm{c}-T_\mathrm{r}\right)+\dfrac{P_0}{\mu_\mathrm{c}}n_\mathrm{r}, \\ \dfrac{\mathrm{d}T_\mathrm{d}}{\mathrm{d}t} = -\dfrac{2M_\mathrm{p}}{\mu_\mathrm{d}}\left(T_\mathrm{d}-T_\mathrm{din}\right)+\dfrac{\Omega_\mathrm{cd}}{\mu_\mathrm{d}}\left(T_\mathrm{c}-T_\mathrm{d}\right), \\ \dfrac{\mathrm{d}\rho_\mathrm{r}}{\mathrm{d}t} = G_\mathrm{r}z_\mathrm{r}. \end{cases} \tag{1}$$

where n_r is the relative nuclear power; c_r is the relative concentration of delayed neutron precursor; β is the fraction of delayed fission neutrons; Λ is the effective prompt neutron life time; ρ_r is the reactivity provided by the control rods; λ is the effective radioactive decay constant of the delayed neutron precursor; α_c and α_r are respectively the reactivity coefficients of the fuel and reflector temperatures; P_0 is the rated reactor thermal power; T_c is the average fuel temperature; T_d is the average temperature of the helium inside the pebble-bed; T_d is the temperature of the helium entering into the pebble-bed; $T_{\mathrm{c,m}}$ and $T_{\mathrm{d,m}}$ are initial equilibrium values of T_c and T_d respectively; T_r is the reflector temperature; Ω_cd and Ω_cr are respectively the heat transfer coefficient between the fuel and helium in the pebble-bed and that between the fuel and reflector inside the riser; M_p is the mass flowrate times the heat capacity of the helium inside the primary loop; μ_c and μ_d are respectively the total heat capacities of the fuel or helium inside the pebble-bed; G_r is the differential reactivity worth of the control rod, and z_r is the rod speed signal generated by the corresponding power-level control strategy.

To obtain the state-space model for power-level control design, the deviations of the actual values of n_r, c_r, T_c, T_d, T_din, T_r and ρ_r from their equilibrium values, *i.e.*, $n_{\mathrm{r}0}$, $c_{\mathrm{r}0}$, $T_{\mathrm{c}0}$, $T_{\mathrm{d}0}$, $T_{\mathrm{din}0}$, $T_{\mathrm{r}0}$ and $\rho_{\mathrm{r}0}$ are respectively defined as:

$$\begin{cases} \delta n_{\mathrm{r}} = n_{\mathrm{r}} - n_{\mathrm{r0}}, \\ \delta c_{\mathrm{r}} = c_{\mathrm{r}} - c_{\mathrm{r0}}, \\ \delta T_{\mathrm{c}} = T_{\mathrm{c}} - T_{\mathrm{c0}}, \\ \delta T_{\mathrm{d}} = T_{\mathrm{d}} - T_{\mathrm{d0}}, \\ \delta T_{\mathrm{din}} = T_{\mathrm{din}} - T_{\mathrm{din0}}, \\ \delta T_{\mathrm{r}} = T_{\mathrm{r}} - T_{\mathrm{r0}}, \\ \delta \rho_{\mathrm{r}} = \rho_{\mathrm{r}} - \rho_{\mathrm{r0}}. \end{cases} \tag{2}$$

Moreover, we define:

$$\boldsymbol{x} = \begin{bmatrix} \delta T_{\mathrm{d}} & \delta T_{\mathrm{c}} & \delta n_{\mathrm{r}} & \delta \rho_{\mathrm{r}} & \delta c_{\mathrm{r}} \end{bmatrix}^{\mathrm{T}} \tag{3}$$

$$\boldsymbol{w} = \begin{bmatrix} \delta T_{\mathrm{din}} & \delta T_{\mathrm{r}} \end{bmatrix}^{\mathrm{T}} \tag{4}$$

and:

$$u = G_{\mathrm{r}} z_{\mathrm{r}} \tag{5}$$

Then, the nonlinear state-space model for power-level control design can be written as:

$$\begin{cases} \dot{\boldsymbol{x}} = \boldsymbol{f}(\boldsymbol{x}) + \boldsymbol{g}u + \boldsymbol{G}(\boldsymbol{x})\boldsymbol{w} \\ \boldsymbol{y} = \boldsymbol{h}(\boldsymbol{x}) \end{cases} \tag{6}$$

where:

$$\boldsymbol{f}(\boldsymbol{x}) = \begin{bmatrix} -\dfrac{\Omega_{\mathrm{cd}} + 2M_{\mathrm{p}}}{\mu_{\mathrm{d}}} x_1 + \dfrac{\Omega_{\mathrm{cd}}}{\mu_{\mathrm{d}}} x_2 \\ \dfrac{\Omega_{\mathrm{cd}}}{\mu_{\mathrm{c}}} x_1 - \dfrac{\Omega_{\mathrm{cd}} + \Omega_{\mathrm{cr}}}{\mu_{\mathrm{c}}} x_2 + \dfrac{P_0}{\mu_{\mathrm{c}}} x_3 \\ -\dfrac{\beta}{\Lambda}(x_3 - x_5) + \dfrac{n_{\mathrm{r0}} + x_3}{\Lambda}(\alpha_{\mathrm{c}} x_2 + x_4) \\ 0 \\ \lambda(x_3 - x_5) \end{bmatrix} \tag{7}$$

$$\boldsymbol{g} = \begin{bmatrix} 0 & 0 & 0 & 1 & 0 \end{bmatrix}^{\mathrm{T}} \tag{8}$$

$$\boldsymbol{G}(\boldsymbol{x}) = \begin{bmatrix} \dfrac{2M_{\mathrm{p}}}{\mu_{\mathrm{d}}} & 0 & 0 & 0 & 0 \\ 0 & \dfrac{\Omega_{\mathrm{cr}}}{\mu_{\mathrm{c}}} & \dfrac{\alpha_{\mathrm{r}}}{\Lambda}(n_{\mathrm{r0}} + x_3) & 0 & 0 \end{bmatrix}^{\mathrm{T}} \tag{9}$$

and:

$$\boldsymbol{h}(\boldsymbol{x}) = \begin{bmatrix} x_1 & c_0 x_3 \end{bmatrix}^{\mathrm{T}} \tag{10}$$

It is noted that the heat capacity of the reflector of the MHTGR is so large that δT_{r} changes very slowly and its amplitude is also very small. Moreover, δT_{din} reflects the influence of the other parts of the MHTGR to the reactor core dynamics. Therefore, it is quite reasonable to view $\boldsymbol{w}$ defined in Equation (4) as the disturbance.

2.2. Problem Formulation

Here, define the evaluation signal of System (6) as:

$$\boldsymbol{\zeta} = \boldsymbol{\zeta}(\boldsymbol{x}) \tag{11}$$

where the vector-valued function ζ is smooth. Then the concept of L_2 disturbance attenuator is introduced as follows:

Definition 1 [15]: consider nonlinear System (6) with evaluation Signal (11). Control input u is said to be an L_2 disturbance attenuator if there is a semi-positive smooth function $V(x)$ such that following γ-dissipation inequality is satisfied:

$$\dot{V}(\boldsymbol{x}) + Q(\boldsymbol{x}) \le \frac{1}{2}\left(\gamma^2 \|\boldsymbol{w}\|_2^2 - \|\boldsymbol{\zeta}\|_2^2\right) \tag{12}$$

where $Q(\boldsymbol{x})$ is a semi-positive function; $\|\cdot\|_2$ is the Euclidean norm, and here γ is a positive scalar called the L_2 gain from disturbance w to evaluation signal ζ.

Remark 1: from Inequality (12), when $w \equiv O$:

$$\frac{\mathrm{d}V(\boldsymbol{x})}{\mathrm{d}t} \le -Q(\boldsymbol{x}) - \frac{1}{2}\|\boldsymbol{z}\|_2^2 \le 0 \tag{13}$$

Based upon Inequality (13), it is clear that if $\forall x \in \Gamma = \{x \mid V(x) \equiv 0\}$ satisfies $x \to 0$ as $t \to \infty$, then from Lasalle's invariance principle, the system is asymptotic stable. After introducing the concept of L_2-disturbance attenuator, the problem to be solved in this paper is given as follows:

Problem 1: how to design an L_2-disturbance attenuator for System (6) with evaluation Signal (11)? That is to say, how to design a power-level controller for the MHTGR with L_2-disturbance attenuation performance?

3. Power-Level Control Based on Iterative Damping Assignment

As we have discussed above, instead of the classical control design techniques that try to impose some predetermined dynamic behavior—usually through nonlinearity cancellation and high gain, the control design based on feedback dissipation is an ever increasing predominance of control techniques. However, the existing feedback dissipation approach such as energy shaping (ES), interconnection and damping assignment passivity based control (IDA-PBC) and etc. usually need System (6) to satisfy the following matching condition:

$$\boldsymbol{h}(\boldsymbol{x}) = \boldsymbol{g}^{\mathrm{T}} \nabla H(\boldsymbol{x}) \tag{14}$$

where H is a semi-positive function called Hamiltonian function. Moreover, the control design by the existing feedback dissipation approach certainly leads to solve a set of partial differential equations.

From Equations (8,10), the dimensions of vectors h and g imply that matching Condition (14) cannot be satisfied here. Furthermore, solving partial differential equations may also lead to intensive complexity. Thus, in this section, the damping assignment is performed by state-feedback iteratively. In the following, the concept of feedback dissipation is firstly introduced. The power-level control (PLC) is then designed through the approach of iterative damping assignment (IDA). Finally, the closed-loop stability and L_2-disturbance attenuation performance of the IDA-PLC are both verified.

3.1. Introduction to the Concept of Feedback Dissipation Control

To introduce the concept of the feedback dissipation control, the concept of the dissipative system is firstly given as follows:

Definition 2: consider the following nonlinear autonomous system:

$$\dot{\chi} = \omega(\chi) \tag{15}$$

where $\chi \in R^n$ and $\omega(O) = O$. If there exists a smooth function $\Gamma(\cdot)$: $R^n \to R^+ = [0, \infty)$ called Hamiltonian function so that inequality is satisfied:

$$\dot{\Gamma}(\chi) = \frac{\partial \Gamma}{\partial \chi}\omega(\chi) \le 0 \tag{16}$$

Then System (15) is said to be a dissipative system corresponding to Hamiltonian function Γ. Moreover, if Inequality (16) holds strictly, then System (15) is strictly dissipative. After introducing the dissipative system, the concept of the generalized Hamiltonian realization is given as follows:

Definition 3: System (15) is called to have a generalized Hamiltonian realization (GHR) if there is a suitable subsets of R^n such that System (15) can be expressed as:

$$\dot{\chi} = T(\chi)\nabla\Gamma(\chi) \tag{17}$$

where $\nabla\Gamma = \left(\frac{\partial \Gamma}{\partial \chi}\right)^{\mathrm{T}}$,and $T \in R^{n\times n}$ is called the structure matrix. Moreover, if structure matrix T can be written as:

$$T(\chi) = J(\chi) - R(\chi) \tag{18}$$

with skew-symmetric J and symmetric nonnegative definite R.

Remark 2: if the structure matrix of System (15) can be represented as Equation (18), then it is dissipative. Moreover, if symmetric matrix R is strict positive definite, then System (15) is strict dissipative.

From Definition 2, system dissipation means shrinkage of a given Hamiltonian function. However, not all of the dynamic systems are dissipative for a given Hamiltonian function, it is reasonable to force a system to be dissipative by the means of feedback. This leads to the definition of feedback dissipation control given as follows:

Definition 4: consider the following nonlinear system:

$$\begin{cases} \dot{\chi} = \omega(\chi) + \zeta(\chi)\upsilon \\ \theta = \eta(\chi) \end{cases} \tag{19}$$

where $\chi \in R^n$ is the system state vector; $\nu \in R^p$ is the control input; $\theta \in R^m$ is the system output, and $\omega(O) = O$. For a given Hamiltonian function $\Gamma(\chi)$, feedback control υ is called a feedback dissipation control if Inequality (20) is satisfied:

$$\dot{\Gamma}(z) = \frac{\partial \Gamma(z)}{\partial z}\left[\omega(z) + \zeta(z)\upsilon\right] \le 0 \tag{20}$$

If Inequality (20) is strictly satisfied, then υ is called a strict feedback dissipation control. If $\upsilon = \upsilon(\chi)$, then it is a state-feedback dissipation control. If $\upsilon = \upsilon(\theta)$, then it is called an output-feedback

dissipation control. Finally, in order for the closed-loop stability analysis, the concepts of zero-state detectability and observability are introduced as follows:

Definition 5 [15]: consider nonlinear System (19), and System (19) is called zero-state detectable if $\theta \equiv O$ and $\upsilon \equiv O$ ($\forall t \geq 0$) implies:

$$\lim_{t \to +\infty} \boldsymbol{z}(t) = \boldsymbol{O} \tag{21}$$

Moreover, this system is called zero-state observable if $\theta \equiv O$ and $\upsilon \equiv O$ implies $z(t) \equiv O$ for $\forall t \geq 0$.

3.2. Design of the Power-Level Control Based on Iterative Damping Assignment

Firstly, we adopt the following the state transformation:

$$\begin{cases} z_i = x_i, i = 1,2,3,5 \\ z_4 = (n_{\mathrm{r0}} + x_3) x_4 \end{cases} \tag{22}$$

and then reactor Dynamics (6) can be rewritten as:

$$\begin{cases} \dot{\boldsymbol{z}} = \bar{\boldsymbol{f}}(\boldsymbol{z}) + \bar{\boldsymbol{g}}(\boldsymbol{z}) u + \bar{\boldsymbol{G}}(\boldsymbol{z}) \boldsymbol{w} \\ \boldsymbol{y} = \bar{\boldsymbol{h}}(\boldsymbol{z}) \end{cases} \tag{23}$$

where:

$$\bar{\boldsymbol{f}}(\boldsymbol{z}) = \begin{bmatrix} -\dfrac{\Omega_{\mathrm{cd}} + 2M_{\mathrm{p}}}{\mu_{\mathrm{d}}} z_1 + \dfrac{\Omega_{\mathrm{cd}}}{\mu_{\mathrm{d}}} z_2 \\ \dfrac{\Omega_{\mathrm{cd}}}{\mu_{\mathrm{c}}} z_1 - \dfrac{\Omega_{\mathrm{cd}} + \Omega_{\mathrm{cr}}}{\mu_{\mathrm{c}}} z_2 + \dfrac{P_0}{\mu_{\mathrm{c}}} z_3 \\ -\dfrac{\beta}{\Lambda}(z_3 - z_5) + \dfrac{\alpha_{\mathrm{c}}}{\Lambda}(n_{\mathrm{r0}} + z_3) z_2 + \dfrac{z_4}{\Lambda} \\ -\dfrac{\beta z_4 (z_3 - z_5)}{\Lambda(n_{\mathrm{r0}} + z_3)} + \dfrac{\alpha_{\mathrm{c}}}{\Lambda} z_2 z_4 + \dfrac{z_4^2}{\Lambda(n_{\mathrm{r0}} + z_3)} \\ \lambda(z_3 - z_5) \end{bmatrix} \tag{24}$$

$$\bar{\boldsymbol{g}}(\boldsymbol{z}) = \begin{bmatrix} 0 & 0 & 0 & n_{\mathrm{r0}} + z_3 & 0 \end{bmatrix}^{\mathrm{T}} \tag{25}$$

$$\bar{\boldsymbol{G}}(\boldsymbol{z}) = \begin{bmatrix} \dfrac{2M_{\mathrm{p}}}{\mu_{\mathrm{d}}} & 0 & 0 & 0 & 0 \\ 0 & \dfrac{\Omega_{\mathrm{cr}}}{\mu_{\mathrm{c}}} & \dfrac{\alpha_{\mathrm{r}}}{\Lambda}(n_{\mathrm{r0}} + z_3) & \dfrac{\alpha_{\mathrm{r}}}{\Lambda} z_4 & 0 \end{bmatrix}^{\mathrm{T}} \tag{26}$$

and:

$$\bar{\boldsymbol{h}}(\boldsymbol{z}) = \begin{bmatrix} z_1 & c_0 z_3 \end{bmatrix}^{\mathrm{T}} \tag{27}$$

In the following, the iterative damping assignment for system (23) is done through state-feedback dissipation step by step:

Step 1:

Define:

$$\begin{cases} \xi_i = z_i, (i = 1,2) \\ \xi_3 = z_3 + \dfrac{2\Omega_{\mathrm{cd}}}{P_0} z_1 \end{cases} \tag{28}$$

and then reactor dynamics can be rewritten as:

$$\begin{cases} \dot{\boldsymbol{\xi}}_1 = (\boldsymbol{J}_1 - \boldsymbol{R}_1)\nabla_{\xi_1} H(\boldsymbol{\xi}_1) + \boldsymbol{p}_1 \xi_3 + \boldsymbol{P}_1 \boldsymbol{w} \\ \dot{\boldsymbol{z}}_1 = \bar{\boldsymbol{f}}_1(\boldsymbol{z}_1) + \bar{\boldsymbol{g}}_1(\boldsymbol{z}_1) u + \bar{\boldsymbol{G}}_1(\boldsymbol{z}) \boldsymbol{w} \end{cases} \tag{29}$$

where:

$$\boldsymbol{\xi}_1 = \begin{bmatrix} \xi_1 & \xi_2 \end{bmatrix}^{\mathrm{T}}$$

$$H_1(\boldsymbol{\xi}_1) = \frac{\xi_1^2}{2\mu_{\mathrm{c}}} + \frac{\xi_2^2}{2\mu_{\mathrm{d}}}$$

$$\boldsymbol{J}_1 = \Omega_{\mathrm{cd}} \begin{bmatrix} 0 & 1 \\ -1 & 0 \end{bmatrix}$$

$$\boldsymbol{R}_1 = \begin{bmatrix} -\mu_{\mathrm{c}} \mu_{\mathrm{d}}^{-1} (\Omega_{\mathrm{cd}} + 2M_{\mathrm{p}}) & 0 \\ 0 & -\mu_{\mathrm{c}}^{-1} \mu_{\mathrm{d}} (\Omega_{\mathrm{cd}} + \Omega_{\mathrm{cr}}) \end{bmatrix}$$

$$\boldsymbol{p}_1 = \begin{bmatrix} 0 & \mu_{\mathrm{c}}^{-1} P_0 \end{bmatrix}^{\mathrm{T}}$$

$$\boldsymbol{P}_1 = \begin{bmatrix} 2\mu_{\mathrm{d}}^{-1} M_{\mathrm{p}} & 0 \\ 0 & \mu_{\mathrm{c}}^{-1} \Omega_{\mathrm{cr}} \end{bmatrix}$$

$$\bar{\boldsymbol{f}}_1(\boldsymbol{z}) = \begin{bmatrix} -\Lambda^{-1}\beta(z_3 - z_5) + \Lambda^{-1}\alpha_{\mathrm{c}}(n_{\mathrm{r0}} + z_3) z_2 + \Lambda^{-1} z_4 \\ \Lambda^{-1}(n_{\mathrm{r0}} + z_3)^{-1} \left[z_4^2 - \beta z_4 (z_3 - z_5) \right] + \Lambda^{-1} \alpha_{\mathrm{c}} z_2 z_4 \\ \lambda(z_3 - z_5) \end{bmatrix}$$

$$\bar{\boldsymbol{g}}_1(\boldsymbol{z}) = \begin{bmatrix} 0 & n_{\mathrm{r0}} + z_3 & 0 \end{bmatrix}^{\mathrm{T}}$$

$$\bar{\boldsymbol{G}}_1(\boldsymbol{z}) = \begin{bmatrix} 0 & 0 & 0 \\ \dfrac{\alpha_{\mathrm{r}}}{\Lambda}(n_{\mathrm{r0}} + z_3) & \dfrac{\alpha_{\mathrm{r}}}{\Lambda} z_4 & 0 \end{bmatrix}^{\mathrm{T}}$$

We can see from the first equation of Equation (29) that it already has the form like a GHR. Next, we shall do like this iteratively.

Step 2:

Based on coordinate Transformation (28), define:

$$\xi_4 = z_4 + C_1 z_1 + C_2 z_2 + \alpha_c z_2 z_3 + \beta z_5 \tag{30}$$

where:

$$C_1 = \frac{2\Omega_{cd}}{P_0}\left(\beta - \frac{\Omega_{cd} + 2M_p}{\mu_d}\Lambda\right) \tag{31}$$

and:

$$C_2 = n_{r0}\alpha_c + \frac{2\Lambda\Omega_{cd}^2}{\mu_d P_0} + \frac{\Lambda P_0}{\mu_c \mu_d} \tag{32}$$

From Equations (28,30), the reactor dynamics can be transformed to:

$$\begin{cases} \dot{\boldsymbol{\xi}}_2 = (\boldsymbol{J}_2 - \boldsymbol{R}_2)\nabla_{\xi_2} H(\boldsymbol{\xi}_2) + \boldsymbol{p}_2 \xi_4 + \boldsymbol{P}_2(z)\boldsymbol{w}, \\ \dot{z}_2 = \bar{\boldsymbol{f}}_2(z_2) + \bar{\boldsymbol{g}}_2(z_2)u + \bar{\boldsymbol{G}}_2(z)\boldsymbol{w}, \end{cases} \tag{33}$$

where:

$$\boldsymbol{\xi}_2 = \begin{bmatrix} \xi_1 & \xi_2 & \xi_3 \end{bmatrix}^T$$

$$H_2(\boldsymbol{\xi}_2) = \frac{\xi_1^2}{2\mu_c} + \frac{\xi_2^2}{2\mu_d} + \frac{\xi_3^2}{2}$$

$$\boldsymbol{J}_2 = \begin{bmatrix} 0 & \Omega_{cd} & 0 \\ -\Omega_{cd} & 0 & \mu_c^{-1} P_0 \\ 0 & -\mu_c^{-1} P_0 & 0 \end{bmatrix}$$

$$\boldsymbol{R}_2 = \begin{bmatrix} \mu_c \mu_d^{-1}(\Omega_{cd} + 2M_p) & 0 & 0 \\ 0 & \mu_c^{-1}\mu_d(\Omega_{cd} + \Omega_{cr}) & 0 \\ 0 & 0 & \Lambda^{-1}\beta \end{bmatrix}$$

$$\boldsymbol{p}_2 = \begin{bmatrix} 0 & 0 & \Lambda^{-1} \end{bmatrix}^T$$

$$\boldsymbol{P}_2(z) = \begin{bmatrix} 2\mu_d^{-1} M_p & 0 & 4(\mu_d P_0)^{-1}\Omega_{cd} M_p \\ 0 & \mu_c^{-1}\Omega_{cr} & \Lambda^{-1}\alpha_r(n_{r0} + z_3) \end{bmatrix}^T$$

$$\bar{\boldsymbol{f}}_2(z) = \begin{bmatrix} \Lambda^{-1}(n_{r0} + z_3)^{-1}\left[z_4^2 - \beta z_4(z_3 - z_5)\right] + \Lambda^{-1}\alpha_c z_2 z_4 \\ \lambda(z_3 - z_5) \end{bmatrix}$$

$$\bar{\boldsymbol{g}}_2(z) = \begin{bmatrix} n_{r0} + z_3 & 0 \end{bmatrix}^T$$

$$\bar{\boldsymbol{G}}_2(z) = \begin{bmatrix} 0 & \frac{\alpha_r}{\Lambda} z_4 \\ 0 & 0 \end{bmatrix}$$

Step 3:

Based on Equation (33), we choose the feedback control u as:

$$u(\boldsymbol{z}) = (n_{r0} + z_3)^{-1} \left\{ \frac{\beta}{\Lambda} \left(\frac{z_4}{n_{r0} + z_3} + \alpha_c z_2 - \lambda \Lambda \right) (z_3 - z_5) - \frac{2\alpha_c}{\Lambda} z_2 z_4 - \frac{\alpha_c^2}{\Lambda} (n_{r0} + z_3) z_2^2 - \frac{\alpha_c P_0}{\mu_c} z_3^2 - \right.$$
$$\frac{\alpha_c \Omega_{cd}}{\mu_c} z_1 z_3 - \alpha_c \left(\sigma\kappa - \frac{\Omega_{cd} + \Omega_{cr}}{\mu_c} \right) z_2 z_3 - \frac{z_4^2}{\Lambda (n_{r0} + z_3)} - D_1 z_1 - D_2 z_2 - D_3 z_3 - \quad (34)$$
$$\left. \sigma\kappa (z_4 + \beta z_5) + v \right\}$$

where:

$$D_1 = \frac{2\Omega_{cd}}{\sigma \Lambda P_0} + \sigma\kappa C_1 + \frac{\Omega_{cd}}{\mu_c} C_2 - \frac{\Omega_{cd} + 2M_p}{\mu_d} C_1 \quad (35)$$

$$D_2 = \frac{\Omega_{cd}}{\mu_d} C_1 + \sigma\kappa C_2 - \frac{\Omega_{cd} + \Omega_{cr}}{\mu_c} \quad (36)$$

$$D_3 = \frac{C_2 P_0}{\mu_c} + \frac{1}{\sigma\Lambda} \quad (37)$$

where v is the compensation term to be designed for guaranteeing the dissipation or stability characteristics of the closed-loop system, and here both κ and σ are given positive scalars.

Substituting control law Equation (33) to Equation (34), we can obtain:

$$\begin{cases} \dot{\boldsymbol{\xi}} = (\boldsymbol{J} - \boldsymbol{R}) \nabla_{\xi} H(\boldsymbol{\xi}) + \boldsymbol{p} v + \boldsymbol{P}(\boldsymbol{z}) \boldsymbol{w} \\ \dot{z}_5 = \lambda (z_3 - z_5) \end{cases} \quad (38)$$

where:

$$\boldsymbol{\xi} = \begin{bmatrix} \xi_1 & \xi_2 & \xi_3 & \xi_4 \end{bmatrix}^T \quad (39)$$

$$H(\boldsymbol{\xi}) = \frac{\xi_1^2}{2\mu_c} + \frac{\xi_2^2}{2\mu_d} + \frac{\xi_3^2}{2} + \frac{\sigma\xi_4^2}{2} \quad (40)$$

$$\boldsymbol{J} = \begin{bmatrix} 0 & \Omega_{cd} & 0 & 0 \\ -\Omega_{cd} & 0 & \mu_c^{-1} P_0 & 0 \\ 0 & -\mu_c^{-1} P_0 & 0 & \sigma^{-1}\Lambda^{-1} \\ 0 & 0 & -\sigma^{-1}\Lambda^{-1} & 0 \end{bmatrix} \quad (41)$$

$$\boldsymbol{R} = \begin{bmatrix} \mu_c \mu_d^{-1} (\Omega_{cd} + 2M_p) & 0 & 0 & 0 \\ 0 & \mu_c^{-1} \mu_d (\Omega_{cd} + \Omega_{cr}) & 0 & 0 \\ 0 & 0 & \Lambda^{-1}\beta & 0 \\ 0 & 0 & 0 & \kappa \end{bmatrix} \quad (42)$$

$$\boldsymbol{p} = \begin{bmatrix} 0 & 0 & 0 & 1 \end{bmatrix}^T \quad (43)$$

$$\boldsymbol{P}(z)=\begin{bmatrix} 2\mu_{\mathrm{d}}^{-1}M_{\mathrm{p}} & 0 & 4\left(\mu_{\mathrm{d}}P_0\right)^{-1}\Omega_{\mathrm{cd}}M_{\mathrm{p}} & 2\mu_{\mathrm{d}}^{-1}M_{\mathrm{p}}C_1 \\ 0 & \mu_{\mathrm{c}}^{-1}\Omega_{\mathrm{cr}} & \Lambda^{-1}\alpha_{\mathrm{r}}\left(n_{\mathrm{r}0}+z_3\right) & p_{42}(z) \end{bmatrix}^{\mathrm{T}} \tag{44}$$

$$p_{42}(z)=\Lambda^{-1}\alpha_{\mathrm{r}}z_4+\mu_{\mathrm{c}}^{-1}\Omega_{\mathrm{cr}}\left(C_2+\alpha_{\mathrm{c}}z_3\right)+\Lambda^{-1}\alpha_{\mathrm{c}}\alpha_{\mathrm{r}}z_2\left(n_{\mathrm{r}0}+z_3\right). \tag{45}$$

From Equations (28,30), the coordinate transformation from z to ξ can be expressed as:

$$\begin{cases} \xi_i=z_i,(i=1,2), \\ \xi_3=z_3+\dfrac{2\Omega_{\mathrm{cd}}}{P_0}z_1, \\ \xi_4=z_4+C_1z_1+C_2z_2+\alpha_{\mathrm{c}}z_2z_3+\beta z_5. \end{cases} \tag{46}$$

Moreover, from Equations (22,46), it is clear that the transformation from x to ξ is:

$$\begin{cases} \xi_i=x_i,(i=1,2), \\ \xi_3=x_3+\dfrac{2\Omega_{\mathrm{cd}}}{P_0}x_1, \\ \xi_4=\left(n_{\mathrm{r}0}+x_3\right)x_4+C_1x_1+C_2x_2+\alpha_{\mathrm{c}}x_2x_3+\beta x_5. \end{cases} \tag{47}$$

Under coordinate x, feedback law Equation (34) can be written as:

$$\begin{aligned} u(\boldsymbol{x})=\left(n_{\mathrm{r}0}+x_3\right)^{-1}\Bigg\{&\frac{\beta}{\Lambda}\left(x_4+\alpha_{\mathrm{c}}x_2-\lambda\Lambda\right)\left(x_3-x_5\right)-\frac{2\alpha_{\mathrm{c}}}{\Lambda}\left(n_{\mathrm{r}0}+x_3\right)x_2x_4-\frac{\alpha_{\mathrm{c}}^2}{\Lambda}\left(n_{\mathrm{r}0}+x_3\right)x_2^2- \\ &\frac{\alpha_{\mathrm{c}}P_0}{\mu_{\mathrm{c}}}x_3^2-\frac{\alpha_{\mathrm{c}}\Omega_{\mathrm{cd}}}{\mu_{\mathrm{c}}}x_1x_3-\alpha_{\mathrm{c}}\left(\sigma\kappa-\frac{\Omega_{\mathrm{cd}}+\Omega_{\mathrm{cr}}}{\mu_{\mathrm{c}}}\right)x_2x_3-\frac{\left(n_{\mathrm{r}0}+x_3\right)x_4^2}{\Lambda}-D_1x_1-D_2x_2- \\ &D_3x_3-\sigma\kappa\left[\left(n_{\mathrm{r}0}+x_3\right)x_4+\beta x_5\right]+v\Bigg\} \end{aligned} \tag{48}$$

The following Proposition 1, which is the first main result of this paper, gives the condition so that feedback law Equation (34) is an L_2 disturbance attenuator corresponding to a given evaluation signal.

Proposition 1: choose the evaluation signal as:

$$\zeta(\boldsymbol{x})=\frac{1}{\sigma}\boldsymbol{p}^{\mathrm{T}}\nabla_{\xi}H(\boldsymbol{\xi})\Big|_{\xi=\xi(\boldsymbol{x})} \tag{49}$$

where ξ, H and p is determined by Equations (40,43,47), respectively. If the compensation term v satisfies:

$$v(\boldsymbol{x})=-K\,\boldsymbol{p}^{\mathrm{T}}\nabla_{\xi}H(\boldsymbol{\xi})\Big|_{\xi=\xi(\boldsymbol{x})} \tag{50}$$

where K is a given positive scalar, then feedback law composed of Equations (48,50) is an L_2 disturbance attenuator corresponding to evaluation signal Equation (49). Moreover, the L_2 gain can be adjusted by feedback gain K. Moreover, if there is no disturbance, *i.e.*:

$$\boldsymbol{w}\equiv\boldsymbol{O} \tag{51}$$

then the closed-loop system is globally asymptotically stable.

Proof: based on the above discussion, it is so clear that differentiating Hamiltonian function Equation (40) along the trajectory given by Equations (6,48,50) is equivalent to that along the trajectory given by Equations (38,50). Then, we can derive that:

$$\begin{aligned}\dot{H}(\boldsymbol{\xi}) &= \nabla_{\boldsymbol{\xi}}^{\mathrm{T}} H(\boldsymbol{\xi})\left[(\boldsymbol{J}-\boldsymbol{R})\nabla_{\boldsymbol{\xi}} H(\boldsymbol{\xi}) + \boldsymbol{p}v + \boldsymbol{P}(z)\boldsymbol{w}\right] \\ &= \nabla_{\boldsymbol{\xi}}^{\mathrm{T}} H(\boldsymbol{\xi})\boldsymbol{J}\nabla_{\boldsymbol{\xi}} H(\boldsymbol{\xi}) - \nabla_{\boldsymbol{\xi}}^{\mathrm{T}} H(\boldsymbol{\xi})\boldsymbol{R}\nabla_{\boldsymbol{\xi}} H(\boldsymbol{\xi}) - K\nabla_{\boldsymbol{\xi}}^{\mathrm{T}} H(\boldsymbol{\xi})\boldsymbol{p}\boldsymbol{p}^{\mathrm{T}}\nabla_{\boldsymbol{\xi}} H(\boldsymbol{\xi}) + \nabla_{\boldsymbol{\xi}}^{\mathrm{T}} H(\boldsymbol{\xi})\boldsymbol{P}(z)\boldsymbol{w} \\ &= -\nabla_{\boldsymbol{\xi}}^{\mathrm{T}} H(\boldsymbol{\xi})\boldsymbol{R}\nabla_{\boldsymbol{\xi}} H(\boldsymbol{\xi}) - K\sigma^2\zeta^2 + \nabla_{\boldsymbol{\xi}}^{\mathrm{T}} H(\boldsymbol{\xi})\boldsymbol{P}(z)\boldsymbol{w} \\ &\le -\left\|\gamma\boldsymbol{w} - \frac{1}{\gamma}\boldsymbol{P}^{\mathrm{T}}(z)\nabla_{\boldsymbol{\xi}} H(\boldsymbol{\xi})\right\|_2^2 - \nabla_{\boldsymbol{\xi}}^{\mathrm{T}} H(\boldsymbol{\xi})\boldsymbol{R}\nabla_{\boldsymbol{\xi}} H(\boldsymbol{\xi}) + \frac{1}{\gamma^2}\nabla_{\boldsymbol{\xi}}^{\mathrm{T}} H(\boldsymbol{\xi})\boldsymbol{P}(z)\boldsymbol{P}^{\mathrm{T}}(z)\nabla_{\boldsymbol{\xi}} H(\boldsymbol{\xi}) + \\ &\frac{1}{2}\left(\gamma^2\|\boldsymbol{w}\|_2^2 - K\sigma^2\zeta^2\right) \\ &\le -\left(\left\|\nabla_{\boldsymbol{\xi}} H(\boldsymbol{\xi})\right\|_{\boldsymbol{R}}^2 - \frac{1}{\gamma}\left\|\nabla_{\boldsymbol{\xi}} H(\boldsymbol{\xi})\right\|_{\boldsymbol{M}(z)}^2\right) + \frac{1}{2}\left(\gamma^2\|\boldsymbol{w}\|_2^2 - K\sigma^2\zeta^2\right)\end{aligned} \tag{52}$$

where:

$$\boldsymbol{M}(z) = \boldsymbol{P}(z)\boldsymbol{P}^{\mathrm{T}}(z) \tag{53}$$

From Equation (42) and Inequality (52), we can properly choose the values of κ and γ such that inequality is satisfied:

$$\left\|\nabla_{\boldsymbol{\xi}} H(\boldsymbol{\xi})\right\|_{\boldsymbol{R}}^2 - \frac{1}{\gamma}\left\|\nabla_{\boldsymbol{\xi}} H(\boldsymbol{\xi})\right\|_{\boldsymbol{M}(z)}^2 \ge \tau \tag{54}$$

where τ is a small positive scalar. Based upon Inequalities (52,54), we have:

$$\dot{H}(\boldsymbol{\xi}) + \tau \le \frac{1}{2}\left(\gamma^2\|\boldsymbol{w}\|_2^2 - K\sigma^2\zeta^2\right) \tag{55}$$

By the use of Inequality (55) and Definition 1, we can easily see that the feedback law composed of Equations (48,50) is an L_2 attenuator of system Equation (6) corresponding to evaluation signal Equation (49). Moreover, from Inequality (55), the L_2 gain from disturbance $\boldsymbol{w}$ to evaluation signal ζ is:

$$\gamma_{L_2} = \frac{\gamma}{\sigma\sqrt{K}} \tag{56}$$

which means that the influence of w to ζ can be effectively reduced by choosing a large K or a large σ. In the following, we shall prove the globally asymptotic closed-loop stability when Condition (51) is satisfied. It is clear that if Equation (51) holds, we have:

$$\begin{aligned}\dot{H}(\boldsymbol{\xi}) &= \nabla_{\boldsymbol{\xi}}^{\mathrm{T}} H(\boldsymbol{\xi})\boldsymbol{J}\nabla_{\boldsymbol{\xi}} H(\boldsymbol{\xi}) - \nabla_{\boldsymbol{\xi}}^{\mathrm{T}} H(\boldsymbol{\xi})\boldsymbol{R}\nabla_{\boldsymbol{\xi}} H(\boldsymbol{\xi}) - K\nabla_{\boldsymbol{\xi}}^{\mathrm{T}} H(\boldsymbol{\xi})\boldsymbol{g}\boldsymbol{g}^{\mathrm{T}}\nabla_{\boldsymbol{\xi}} H(\boldsymbol{\xi}) \\ &= -\left\|\nabla_{\boldsymbol{\xi}} H(\boldsymbol{\xi})\right\|_{\boldsymbol{R}}^2 - K\sigma^2\xi_4^2 \\ &= -\left\|\nabla_{\boldsymbol{\xi}} H(\boldsymbol{\xi})\right\|_{\bar{\boldsymbol{R}}}^2 \le 0\end{aligned} \tag{57}$$

where:

$$\bar{\boldsymbol{R}} = \begin{bmatrix} \mu_{\mathrm{c}}\mu_{\mathrm{d}}^{-1}\left(\Omega_{\mathrm{cd}} + 2M_{\mathrm{p}}\right) & 0 & 0 & 0 \\ 0 & \mu_{\mathrm{c}}^{-1}\mu_{\mathrm{d}}\left(\Omega_{\mathrm{cd}} + \Omega_{\mathrm{cr}}\right) & 0 & 0 \\ 0 & 0 & \Lambda^{-1}\beta & 0 \\ 0 & 0 & 0 & \kappa + K \end{bmatrix} \tag{58}$$

From Equations (40,57,58), state-vector x asymptotically converges to the set defined as:

$$\Xi \triangleq \left\{ \boldsymbol{x} \middle| \boldsymbol{\xi}(\boldsymbol{x}) \equiv \boldsymbol{O} \right\} \tag{59}$$

Based upon coordinate Transformation (47), set Ξ is equivalent to:

$$\Xi_1 \triangleq \left\{ \boldsymbol{x} \middle| x_1 = x_2 = x_3 \equiv 0, \quad n_{\mathrm{r0}} x_4 + \beta x_5 \equiv 0 \right\} \tag{60}$$

Moreover, from Equations (6,7), for $\forall x \in \Xi_1$, it is quite clear that:

$$\lim_{t \to \infty} \boldsymbol{x}(t) = \boldsymbol{O}$$

which manifests that the closed-loop system is globally asymptotically stable if $w \equiv O$. This completes the proof of this proposition.

Remark 3: based on Inequality (57) and Equation (58), when there is no disturbance, the closed-loop system is still globally asymptotically stable even if $K = 0$. That is to say, feedback law Equation (34) with $v = 0$ is enough to guarantee the globally asymptotic closed-loop stability in case of $w \equiv O$.

Remark 4: from Equations (40,43,47), it is easily to see that:

$$\zeta(\boldsymbol{x}) = \xi_4(\boldsymbol{x}) = (n_{\mathrm{r0}} + x_3) x_4 + C_1 x_1 + C_2 x_2 + \alpha_{\mathrm{c}} x_2 x_3 + \beta x_5 \tag{61}$$

and:

$$v(\boldsymbol{x}) = -\sigma K \xi_4(\boldsymbol{x}) = -\sigma K \left[(n_{\mathrm{r0}} + x_3) x_4 + C_1 x_1 + C_2 x_2 + \alpha_{\mathrm{c}} x_2 x_3 + \beta x_5 \right] \tag{62}$$

Substituting Equation (48) to Equation (62), we can get the total feedback control law, *i.e.*,

$$\begin{aligned} u(\boldsymbol{x}) = (n_{\mathrm{r0}} + x_3)^{-1} \Bigg\{ & \frac{\beta}{\Lambda} (x_4 + \alpha_{\mathrm{c}} x_2 - \lambda \Lambda)(x_3 - x_5) - \frac{2\alpha_{\mathrm{c}}}{\Lambda} (n_{\mathrm{r0}} + x_3) x_2 x_4 - \frac{\alpha_{\mathrm{c}}^2}{\Lambda} (n_{\mathrm{r0}} + x_3) x_2^2 - \\ & \frac{\alpha_{\mathrm{c}} P_0}{\mu_{\mathrm{c}}} x_3^2 - \frac{\alpha_{\mathrm{c}} \Omega_{\mathrm{cd}}}{\mu_{\mathrm{c}}} x_1 x_3 - \alpha_{\mathrm{c}} \left[\sigma \bar{K} - \frac{\Omega_{\mathrm{cd}} + \Omega_{\mathrm{cr}}}{\mu_{\mathrm{c}}} \right] x_2 x_3 - \frac{(n_{\mathrm{r0}} + x_3) x_4^2}{\Lambda} - \bar{D}_1 x_1 - \bar{D}_2 x_2 - \\ & D_3 x_3 - \sigma \bar{K} \left[(n_{\mathrm{r0}} + x_3) x_4 + \beta x_5 \right] \Bigg\} \end{aligned} \tag{63}$$

where:

$$\bar{K} = K + \kappa \tag{64}$$

$$\bar{D}_1 = \frac{2\Omega_{\mathrm{cd}}}{\sigma \Lambda P_0} + \sigma \bar{K} C_1 + \frac{\Omega_{\mathrm{cd}}}{\mu_{\mathrm{c}}} C_2 - \frac{\Omega_{\mathrm{cd}} + 2M_{\mathrm{p}}}{\mu_{\mathrm{d}}} C_1 \tag{65}$$

$$\bar{D}_2 = \frac{\Omega_{\mathrm{cd}}}{\mu_{\mathrm{d}}} C_1 + \sigma \bar{K} C_2 - \frac{\Omega_{\mathrm{cd}} + \Omega_{\mathrm{cr}}}{\mu_{\mathrm{c}}} \tag{66}$$

It can be easily seen from Equation (63) that the function of this control law is realized through feeding back all the state-variables. Since only x_1 and x_3, *i.e.*, δn_{r} and δT_{d} can be obtained through measurement, it is quite necessary to design a convergent state-observer for the implementation of this newly-built power-level control strategy.

4. Dynamic Output-Feedback Power-Level Control Strategy

In this section, for the implementation of the nonlinear state-feedback power-level controller Equation (63), the corresponding state-observer is designed firstly. Based on this observation strategy, the dynamic output-feedback power-level control law is developed. Through theoretical analysis that will be given in this section, this control strategy can provide power-level regulation function for the MHTGR with the performance of L_2 disturbance attenuation.

4.1. Observation Strategy

The dissipation-based high-gain filter (DHGF) is an asymptotic state-observer for nonlinear systems, which has been proved to satisfy the separation principle. The DHGF is firstly introduced in this sub-section, and then a DHGF is designed for MHTGR dynamics Equation (6) without disturbances.

Consider the following nonlinear dynamic system:

$$\begin{cases} \dot{\boldsymbol{\varsigma}} = \boldsymbol{\psi}(\boldsymbol{\varsigma}) + \boldsymbol{\chi}(\boldsymbol{\varsigma})\boldsymbol{\mu} \\ \boldsymbol{\eta} = \boldsymbol{\varphi}(\boldsymbol{\varsigma}) \end{cases} \tag{67}$$

where $\varsigma \in R^n$ is the state-vector; $\eta \in R^m$ is the system output; $\mu \in R^p$ is the control input and vector-valued functions ψ, φ and χ are all smooth.

Suppose that the state-observer corresponding to System (67) takes the form as:

$$\dot{\hat{\boldsymbol{\varsigma}}} = \boldsymbol{\psi}(\hat{\boldsymbol{\varsigma}}) + \boldsymbol{\chi}(\hat{\boldsymbol{\varsigma}})\boldsymbol{\mu} + \boldsymbol{F}_{\mathrm{O}}\boldsymbol{\tau} \tag{68}$$

where $\hat{\varsigma} \in R^n$ is the state-observation, $F_O \in R^{n\times m}$ is the gain matrix of the observer,

$$\boldsymbol{\tau} = \boldsymbol{\eta} - \hat{\boldsymbol{\eta}} = \boldsymbol{\varphi}(\boldsymbol{\varsigma}) - \boldsymbol{\varphi}(\hat{\boldsymbol{\varsigma}}) \tag{69}$$

and:

$$\hat{\boldsymbol{\eta}} = \boldsymbol{\varphi}(\hat{\boldsymbol{\varsigma}}) \tag{70}$$

Moreover, we define the observation error as:

$$\boldsymbol{\upsilon} = \boldsymbol{\varsigma} - \hat{\boldsymbol{\varsigma}} \tag{71}$$

and then it is clear that the dynamics of the observation error can be written as:

$$\dot{\boldsymbol{\upsilon}} = \boldsymbol{\Psi}(\boldsymbol{\upsilon}, \hat{\boldsymbol{\varsigma}}) - \boldsymbol{F}_{\mathrm{O}}(\boldsymbol{\eta} - \hat{\boldsymbol{\eta}}) \tag{72}$$

where:

$$\boldsymbol{\Psi}(\boldsymbol{\upsilon}, \hat{\boldsymbol{\varsigma}}) = \boldsymbol{\varphi}(\boldsymbol{\varsigma}) - \boldsymbol{\varphi}(\hat{\boldsymbol{\varsigma}}) \tag{73}$$

The following Lemma 1 guarantees not only the convergence of State-observer (68) but also the stability of the closed-loop system composed of Dynamics (67), a stabilizer μ and Observer (68):

Lemma 1 [24,25]: Consider nonlinear system Equation (67) with State-observer Equation (68), and here suppose that:

$$\boldsymbol{\mu} = \boldsymbol{\Phi}(\boldsymbol{\varsigma}) \tag{74}$$

is a state-feedback control law for System (67). Moreover, assume that observation error dynamics Equation (72) with its output defined as Equation (69) is zero-state observable, and there exists a smooth function $\Theta_{\mathrm{O}}(\cdot): R^m \to R^+ \triangleq [0,+\infty)$, which satisfies:

$$\boldsymbol{\tau} = \boldsymbol{B}^{\mathrm{T}} \left[\frac{\partial \Theta_{\mathrm{O}}(\boldsymbol{\tau})}{\partial \boldsymbol{v}} \right]^{\mathrm{T}} \tag{75}$$

and is only minimal at point $\tau = O$. Then state-observer Equation (68) is convergent and dynamic output feedback controller:

$$\begin{cases} \boldsymbol{\mu} = \boldsymbol{\Phi}(\hat{\varsigma}) \\ \dot{\hat{\varsigma}} = \boldsymbol{\psi}(\hat{\varsigma}) + \boldsymbol{\chi}(\hat{\varsigma})\boldsymbol{\Phi}(\hat{\varsigma}) + \boldsymbol{F}_{\mathrm{O}}\boldsymbol{\tau} \end{cases} \tag{76}$$

is also an asymptotic stabilizer if:

$$\boldsymbol{F}_{\mathrm{O}} = \frac{1}{\vartheta}\boldsymbol{B} \tag{77}$$

where ϑ is a small enough positive scalar. The State-observer (68) with its gain matrix satisfying Equation (77) is called the dissipation-based high gain filter (DHGF).

Proof: See References [24,25].

4.2. Design and Analysis of the Dynamic Output-Feedback Power-Level Control Strategy

From the above discussion, it is natural for us to design the state-observer for System (6) as:

$$\dot{\hat{\boldsymbol{x}}} = \boldsymbol{f}(\hat{\boldsymbol{x}}) + \boldsymbol{g}u(\hat{\boldsymbol{x}}) + \boldsymbol{K}_{\mathrm{O}}\left[\boldsymbol{h}(\boldsymbol{x}) - \boldsymbol{h}(\hat{\boldsymbol{x}})\right] \tag{78}$$

where $f(\cdot)$ and g is respectively defined by Equations (7,8), output function $h(\cdot)$ is determined by Equation (10), and control law $u(\cdot)$ is given by Equation (63). Based on Equations (63,78), the corresponding dynamic output feed-back controller can be written as:

$$\begin{cases} u = u(\hat{\boldsymbol{x}}) \\ \dot{\hat{\boldsymbol{x}}} = \boldsymbol{f}(\hat{\boldsymbol{x}}) + \boldsymbol{g}u(\hat{\boldsymbol{x}}) + \boldsymbol{K}_{\mathrm{O}}\left[\boldsymbol{h}(\boldsymbol{x}) - \boldsymbol{h}(\hat{\boldsymbol{x}})\right] \end{cases} \tag{79}$$

where functions $f(\cdot)$, g, $h(\cdot)$ and $u(\cdot)$ respectively have the same meaning with those in Equation (78). Moreover, it is clear that the corresponding observation error dynamics of Equation (78) is:

$$\dot{\boldsymbol{e}} = \boldsymbol{f}_{\mathrm{e}}(\boldsymbol{e}, \hat{\boldsymbol{x}}) - \boldsymbol{K}_{\mathrm{O}}\boldsymbol{e}_y + \boldsymbol{G}(\boldsymbol{x})\boldsymbol{w} \tag{80}$$

where:

$$\boldsymbol{e} = \boldsymbol{x} - \hat{\boldsymbol{x}} \tag{81}$$

$$\boldsymbol{f}(\boldsymbol{e}, \hat{\boldsymbol{x}}) = \boldsymbol{f}(\boldsymbol{x}) - \boldsymbol{f}(\hat{\boldsymbol{x}}) \tag{82}$$

and:

$$\boldsymbol{e}_y = \boldsymbol{h}_{\mathrm{e}}(\boldsymbol{e}) = \boldsymbol{h}(\boldsymbol{x}) - \boldsymbol{h}(\hat{\boldsymbol{x}}) = \begin{bmatrix} e_1 & c_0 e_3 \end{bmatrix}^{\mathrm{T}} \tag{83}$$

Following Proposition 2, which is the second main result in this paper, gives a sufficient condition for dynamic output feedback controller Equation (79) to be an L_2 disturbance attenuator.

Proposition 2: dynamic output feedback controller Equation (79) is an L_2 disturbance attenuator for System (6) if the gain matrix K_O satisfies:

$$\boldsymbol{K}_{\mathrm{O}} = \frac{1}{\varepsilon}\boldsymbol{L} \tag{84}$$

where:

$$\boldsymbol{L} = \begin{bmatrix} 1 & 0 & 0 & 0 & 0 \\ 0 & 0 & 1 & 0 & 0 \end{bmatrix}^{\mathrm{T}} \tag{85}$$

where ε is a small enough positive scalar. Furthermore, if there is no disturbance, *i.e.*, Condition (51) holds, then control strategy Equation (79) is a globally asymptotic stabilizer, and Observer (78) is also convergent.

Proof: Define:

$$H_{\mathrm{O}}\left(\boldsymbol{e}_y\right) = \frac{1}{2}\left(e_1^2 + c_0 e_3^2\right) \tag{86}$$

and it is clear that function $H_O(\cdot)$ is only minimal at $e_y \equiv O$. It is also easily to derive that:

$$\begin{aligned} \boldsymbol{L}^{\mathrm{T}}\left(\frac{\partial H_{\mathrm{O}}\left(\boldsymbol{e}_y\right)}{\partial \boldsymbol{e}}\right)^{\mathrm{T}} &= \left(\frac{\partial H_{\mathrm{O}}\left(\boldsymbol{e}_y\right)}{\partial \boldsymbol{e}}\boldsymbol{L}\right)^{\mathrm{T}} \\ &= \left(\begin{bmatrix} e_1 & 0 & c_0 e_3 & 0 & 0 \end{bmatrix} \cdot \begin{bmatrix} 1 & 0 & 0 & 0 & 0 \\ 0 & 0 & 1 & 0 & 0 \end{bmatrix}^{\mathrm{T}}\right)^{\mathrm{T}} \\ &= \begin{bmatrix} e_1 & c_0 e_3 \end{bmatrix}^{\mathrm{T}} = \boldsymbol{e}_y \end{aligned} \tag{87}$$

which means that Condition (75) is satisfied.

Substituting $e_y \equiv O$ and $w \equiv O$ to observation error dynamics Equation (80), and we have:

$$\begin{cases} 0 = \mu_{\mathrm{d}}^{-1}\Omega_{\mathrm{cd}} e_2, \\ \dot{e}_2 = -\mu_{\mathrm{c}}^{-1}\left(\Omega_{\mathrm{cd}} + \Omega_{\mathrm{cr}}\right)e_2, \\ 0 = \Lambda^{-1}\beta e_5 + \Lambda^{-1}\left(n_{\mathrm{r0}} + x_3\right)\left(\alpha_{\mathrm{c}} e_2 + e_4\right), \\ \dot{e}_4 = 0, \\ \dot{e}_5 = -\lambda e_5. \end{cases} \tag{88}$$

which is equivalent to:

$$\begin{cases} e_i = 0, \quad (i = 1,2,3), \\ \beta e_5 + \left(n_{\mathrm{r0}} + x_3\right)e_4 = 0, \\ \dot{e}_4 = 0, \\ \dot{e}_5 = -\lambda e_5. \end{cases} \tag{89}$$

Since the value of x_3 can be arbitrarily given, it is easily to see from Equation (89) that:

$$\left.\begin{matrix} \boldsymbol{e}_y \equiv \boldsymbol{O} \\ \boldsymbol{w} \equiv \boldsymbol{O} \end{matrix}\right\} \Rightarrow \boldsymbol{e} \equiv \boldsymbol{O} \tag{90}$$

which means that observation error Dynamics (80) under Condition (51) is zero-state observable with its output defined as e_y. Since state-feedback control Equation (48) is a globally asymptotic stabilizer if

Condition (51) is satisfied, it can be seen from Lemma 1, Equations (86,87,90) that control strategy Equation (79) is still a globally asymptotical stabilizer and Observer (78) is convergent under Condition (51).

Next, we shall prove that control law Equation (79) is still an L_2 disturbance attenuator even if $w \neq O$. Define the extended Hamiltonian function for the closed-loop system composed of Equations (6,79) as:

$$\bar{H}\left(\boldsymbol{x},\boldsymbol{e}_y\right)=H\left(\boldsymbol{\xi}\right)\big|_{\xi=\xi(x)}+H_{\mathrm{O}}\left(\boldsymbol{e}_y\right) \tag{91}$$

where functions $H(\cdot)$ and $H_{\mathrm{O}}(\cdot)$ are determined by Equations (40,86), respectively. Differentiating Equation (91) along the trajectory given by Equations (6,79), we can derive that:

$$\begin{aligned}
\dot{\bar{H}}\left(\boldsymbol{x},\boldsymbol{e}_y\right)&=\dot{H}\left(\boldsymbol{\xi}\right)\big|_{u=u(\hat{x})}+\dot{H}_{\mathrm{O}}\left(\boldsymbol{e}_y\right)\\
&=\dot{H}\left(\boldsymbol{\xi}\right)\big|_{u=u(x)}-\left[\boldsymbol{g}^{\mathrm{T}}\nabla_x H\left(\boldsymbol{\xi}\big|_{\xi=\xi(x)}\right)\right]\left[u(\boldsymbol{x})-u(\hat{\boldsymbol{x}})\right]+\nabla_e^{\mathrm{T}}H_{\mathrm{O}}\left(\boldsymbol{e}_y\right)\left[\boldsymbol{f}_{\mathrm{e}}\left(\boldsymbol{e},\hat{\boldsymbol{x}}\right)-\boldsymbol{K}_{\mathrm{O}}\boldsymbol{e}_y+\boldsymbol{G}(\boldsymbol{x})\boldsymbol{w}\right]\\
&=-\left\|\nabla_\xi H\left(\boldsymbol{\xi}\right)\right\|_{\boldsymbol{R}}^2-K\sigma^2\zeta^2+\left[\boldsymbol{P}^{\mathrm{T}}\left(\boldsymbol{z}\right)\nabla_\xi H\left(\boldsymbol{\xi}\right)+\boldsymbol{G}^{\mathrm{T}}\left(\boldsymbol{x}\right)\nabla_e H_{\mathrm{O}}\left(\boldsymbol{e}_y\right)\right]^{\mathrm{T}}\boldsymbol{w}+\nabla_e^{\mathrm{T}}H_{\mathrm{O}}\left(\boldsymbol{e}_y\right)\boldsymbol{f}_{\mathrm{e}}\left(\boldsymbol{e},\hat{\boldsymbol{x}}\right)-\\
&\left[\boldsymbol{g}^{\mathrm{T}}\nabla_x H\left(\boldsymbol{\xi}\big|_{\xi=\xi(x)}\right)\right]\left[u(\boldsymbol{x})-u(\hat{\boldsymbol{x}})\right]-\frac{1}{\varepsilon}\left\|\boldsymbol{e}_y\right\|_2^2\\
&\leq-\left\|\gamma\boldsymbol{w}-\frac{1}{\gamma}\left[\boldsymbol{P}^{\mathrm{T}}\left(\boldsymbol{z}\right)\nabla_\xi H\left(\boldsymbol{\xi}\right)+\boldsymbol{G}^{\mathrm{T}}\left(\boldsymbol{x}\right)\nabla_e H_{\mathrm{O}}\left(\boldsymbol{e}_y\right)\right]\right\|_2^2-\left\|\nabla_\xi H\left(\boldsymbol{\xi}\right)\right\|_{\boldsymbol{R}}^2+\frac{1}{2}\left(\gamma^2\left\|\boldsymbol{w}\right\|_2^2-K\sigma^2\zeta^2\right)+\\
&\frac{1}{\gamma^2}\left\|\boldsymbol{P}^{\mathrm{T}}\left(\boldsymbol{z}\right)\nabla_\xi H\left(\boldsymbol{\xi}\right)+\boldsymbol{G}^{\mathrm{T}}\left(\boldsymbol{x}\right)\nabla_e H_{\mathrm{O}}\left(\boldsymbol{e}_y\right)\right\|_2^2-\left[\boldsymbol{g}^{\mathrm{T}}\nabla_x H\left(\boldsymbol{\xi}\big|_{\xi=\xi(x)}\right)\right]\left[u(\boldsymbol{x})-u(\hat{\boldsymbol{x}})\right]+\\
&\nabla_e^{\mathrm{T}}H_{\mathrm{O}}\left(\boldsymbol{e}_y\right)\boldsymbol{f}_{\mathrm{e}}\left(\boldsymbol{e},\hat{\boldsymbol{x}}\right)-\frac{1}{\varepsilon}\left\|\boldsymbol{e}_y\right\|_2^2\\
&\leq\frac{1}{2}\left(\gamma^2\left\|\boldsymbol{w}\right\|_2^2-K\sigma^2\zeta^2\right)-\left(\left\|\nabla_\xi H\left(\boldsymbol{\xi}\right)\right\|_{\boldsymbol{R}}^2-\frac{1}{\gamma^2}\left\|\boldsymbol{P}^{\mathrm{T}}\left(\boldsymbol{z}\right)\nabla_\xi H\left(\boldsymbol{\xi}\right)+\boldsymbol{G}^{\mathrm{T}}\left(\boldsymbol{x}\right)\nabla_e H_{\mathrm{O}}\left(\boldsymbol{e}_y\right)\right\|_2^2\right)-\\
&\left\{\frac{1}{\varepsilon}\left\|\boldsymbol{e}_y\right\|_2^2+\left[\boldsymbol{g}^{\mathrm{T}}\nabla_x H\left(\boldsymbol{\xi}\big|_{\xi=\xi(x)}\right)\right]\left[u(\boldsymbol{x})-u(\hat{\boldsymbol{x}})\right]-\nabla_e^{\mathrm{T}}H_{\mathrm{O}}\left(\boldsymbol{e}_y\right)\boldsymbol{f}_{\mathrm{e}}\left(\boldsymbol{e},\hat{\boldsymbol{x}}\right)\right\}
\end{aligned} \tag{92}$$

where matrices $\boldsymbol{L}$ and $\boldsymbol{M}$ are respectively defined by Equations (53,85).

From Inequality (92), by properly choosing the values of positive scalars κ, γ and ε, it is easy to guarantee that inequalities:

$$\left\|\nabla_\xi H\left(\boldsymbol{\xi}\right)\right\|_{\boldsymbol{R}}^2-\frac{1}{\gamma^2}\left\|\boldsymbol{P}^{\mathrm{T}}\left(\boldsymbol{z}\right)\nabla_\xi H\left(\boldsymbol{\xi}\right)+\boldsymbol{G}^{\mathrm{T}}\left(\boldsymbol{x}\right)\nabla_e H_{\mathrm{O}}\left(\boldsymbol{e}_y\right)\right\|_2^2\geq\theta_1 \tag{93}$$

$$\frac{1}{\varepsilon}\left\|\boldsymbol{e}_y\right\|_2^2+\left[\boldsymbol{g}^{\mathrm{T}}\nabla_x H\left(\boldsymbol{\xi}\big|_{\xi=\xi(x)}\right)\right]\left[u(\boldsymbol{x})-u(\hat{\boldsymbol{x}})\right]-\nabla_e^{\mathrm{T}}H_{\mathrm{O}}\left(\boldsymbol{e}_y\right)\boldsymbol{f}_{\mathrm{e}}\left(\boldsymbol{e},\hat{\boldsymbol{x}}\right)\geq\theta_2 \tag{94}$$

where θ_1 and θ_2 are both small positive scalars.

From Inequalities (92–94), we find that:

$$\dot{\bar{H}}\left(\boldsymbol{x},\boldsymbol{e}_y\right)+\theta\leq\frac{1}{2}\left(\gamma^2\left\|\boldsymbol{w}\right\|_2^2-K\sigma^2\zeta^2\right) \tag{95}$$

where $\theta=\theta_1+\theta_2$. Based upon Inequality (95) and Definition 1, it is now quite clear that dynamic output feedback control strategy Equation (79) with observer gain Equation (84) and a small enough ε is still a L_2 disturbance attenuator in case of $w \neq O$. This is completes the proof of Proposition 2.

5. Simulation Results with Discussion

To show the feasibility and performance of the dynamic output feedback power-level control law determined by Equations (7,8,10,63,79) this newly developed controller is applied to the power-level regulation of a NSSS of the HTR-PM plant in this section. The influence of the controller parameters to the control performance is also illustrated and analyzed.

5.1. Description of the Numerical Simulation

The numerical simulation model is developed based on Visual C++. Since the height-to-diameter ratio of the HTR-PM reactor is nearly 4, the classical point kinetics model is not suitable for building the simulation code of the reactor core. By dividing the active core region into 10 parts vertically, a nodal neutron kinetics model and its thermal-hydraulic model are utilized to establish the simulation code [27]. The adopted OTSG model is just the classical moving boundary model [28]. The schematic view of the dynamic model of the NSSS for numerical simulation is shown in Figure 2. Furthermore, the model of the steam turbine and that of the electrical generator are also included in the simulation code [29]. The numerical simulation of this paper was done by the use of this simulation code.

Figure 2. Schematic view of the dynamic model of the NSSS.

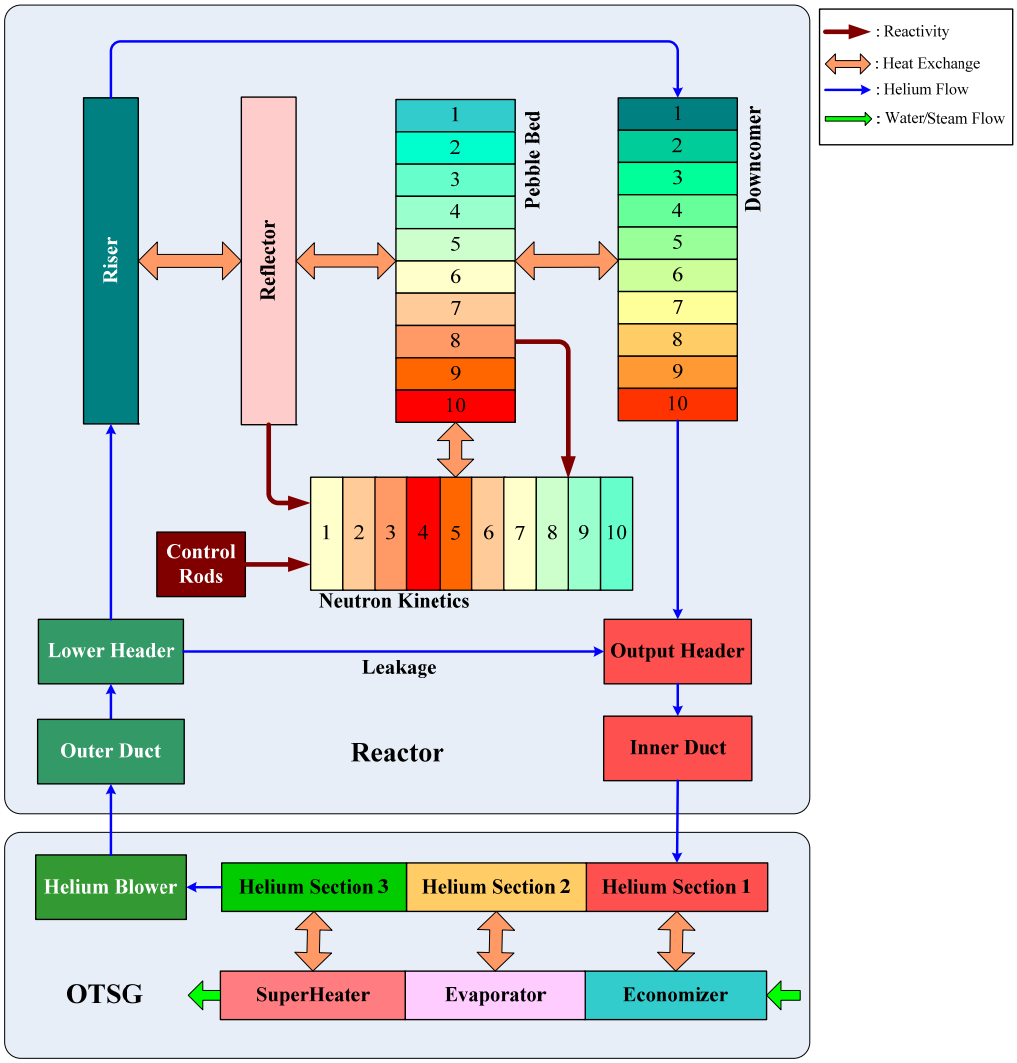

5.2. Simulation Results

In the simulation, the following two case studies are done to show the feasibility and performance of newly-built dynamic output-feedback power-level control law Equation (79):

Case A (large power drop): power-level changes linearly from 100% to 50% in 5 minutes;

Case B (large power lift): power-level changes linearly from 50% to 100% in 5minutes.

From Equations (31,32,37,63,65,66), it is clear that since scalars C_1 and C_2 are so small that the influence of the value of $\bar{K}$ to the control performance is much weaker than that of σ. Therefore, in this study, we only check the influence of parameters σ and ε to the control performance.

Figure 3. Dynamic responses in Case A of (**a**) relative nuclear power; (**b**) average fuel temperature; (**c**) outlet helium temperature and (**d**) control rod speed signal with different σ and constant ε.

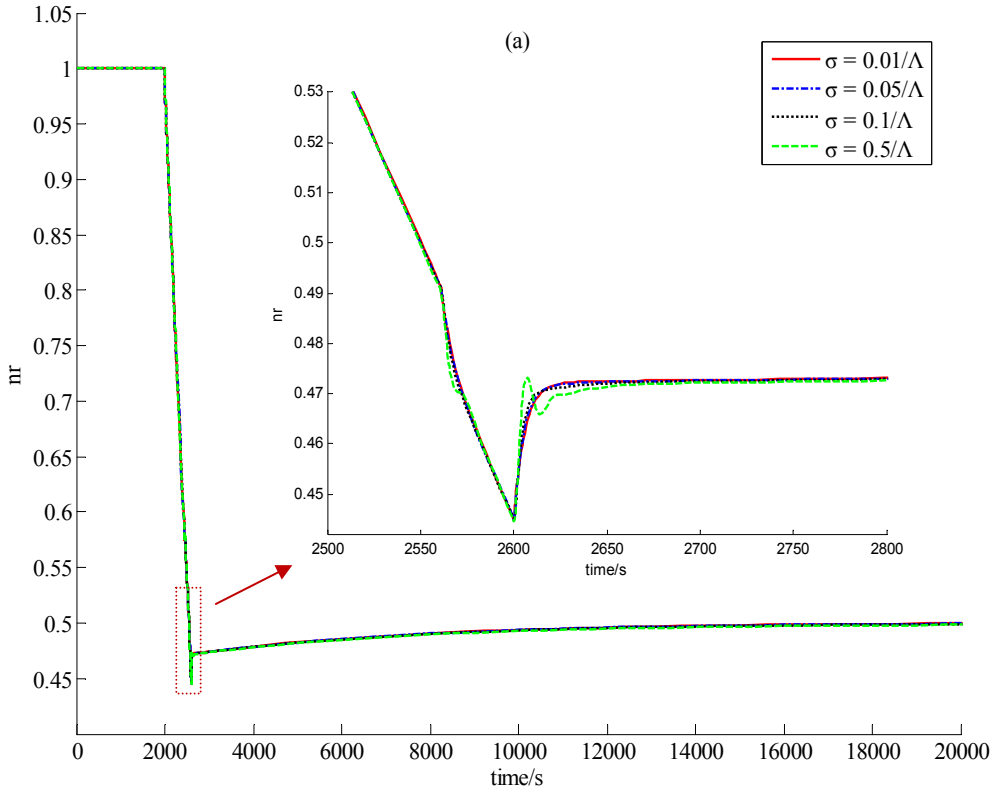

Figure 3. *Cont.*

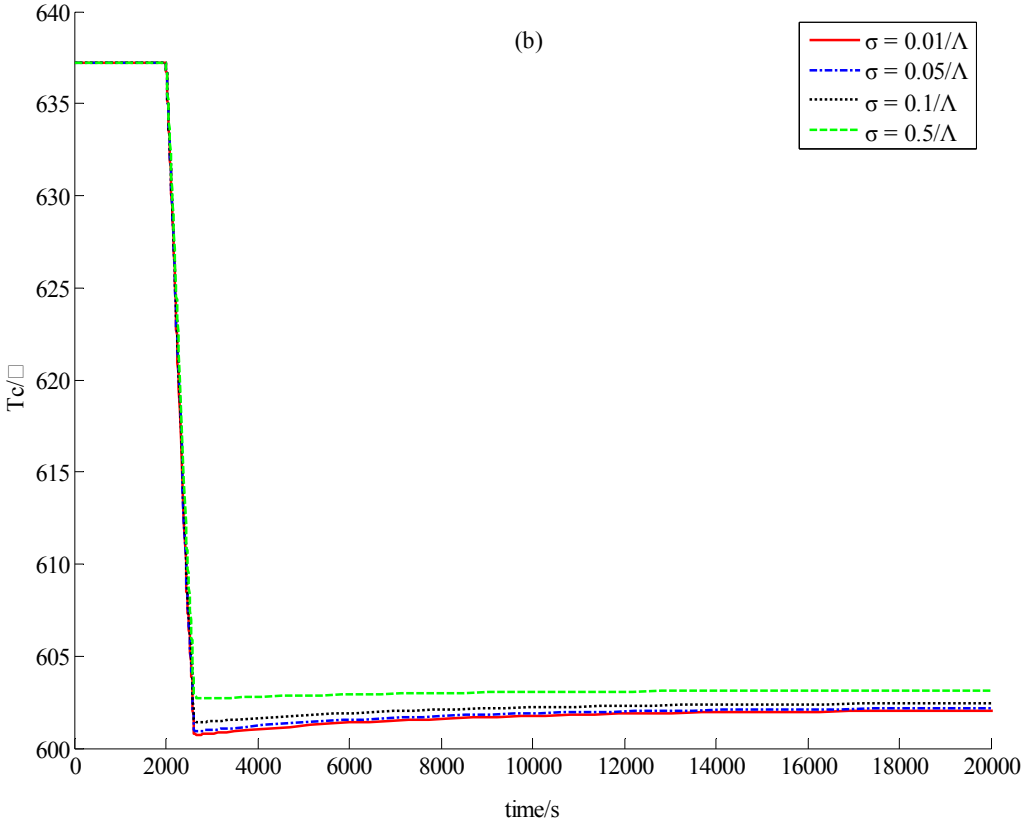

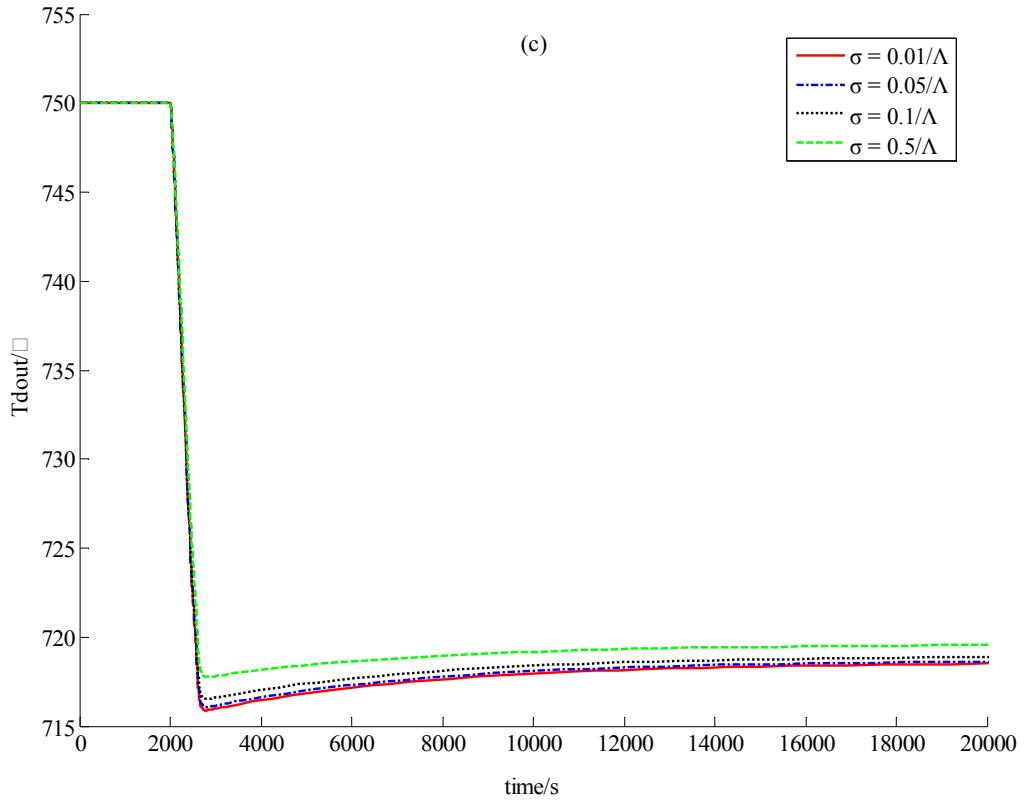

Figure 3. *Cont.*

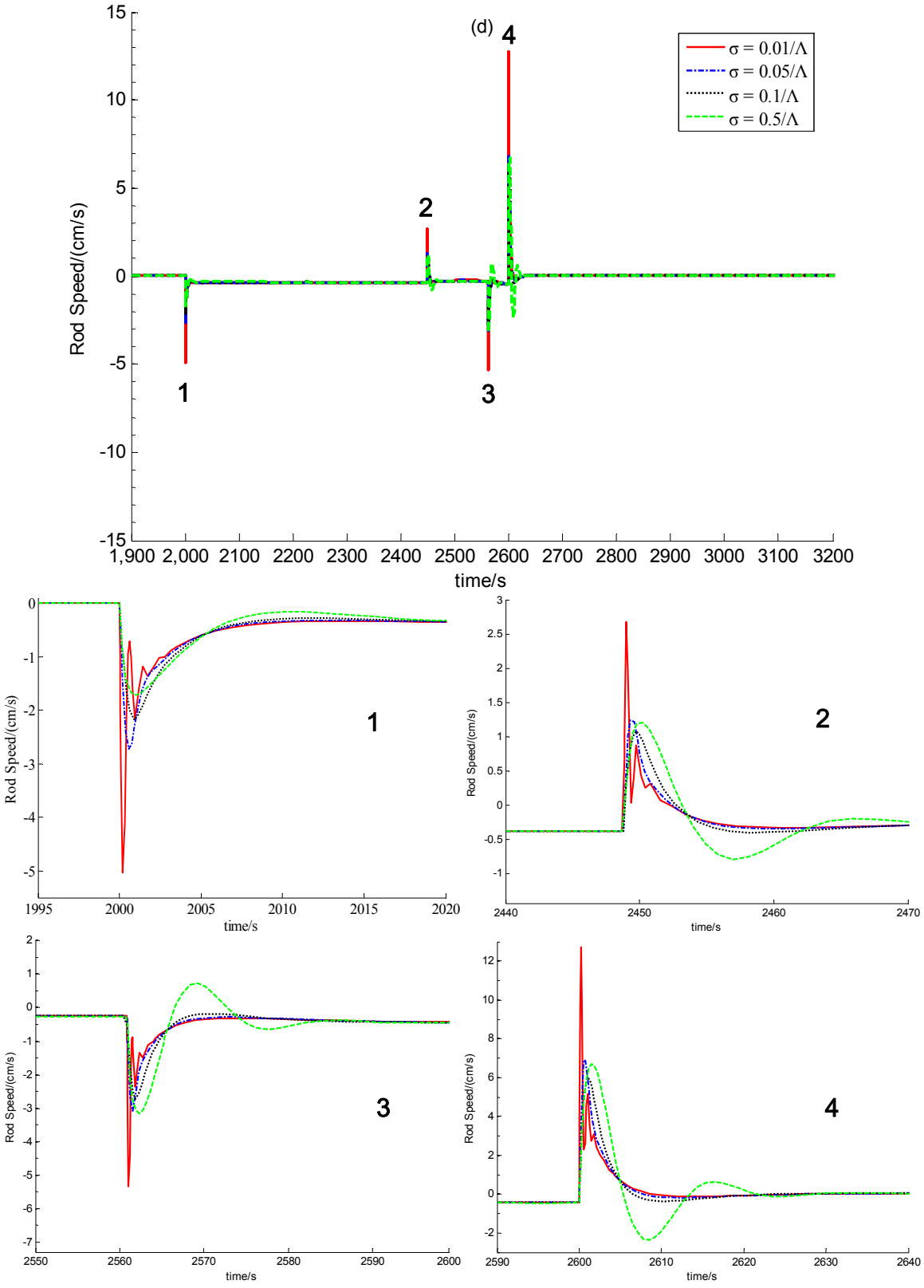

In the numerical simulation, $\bar{K}$ is set to be 10.0, and control parameter σ and observation parameter ε are set to be different values respectively.

Case A: In this test, the power demand signal decreases down from 100% to 50% linearly with a speed of 5%/min. Corresponding to the power demand drop, both the error between the actual and the demanded power-levels and that between the actual and the referenced values of average coolant temperature become larger than before. These error signals stimulate the power-level controller to insert the control rod in order to weaken these two error signals. If scalar ε = 0.01 and σ adopts different values, then the responses of the relative nuclear power, average fuel temperature, average helium temperature and control rod speed generated by power-level controller Equation (79) during the transition period are all illustrated in Figure 3. If scalar $\sigma = 0.01/\Lambda$ and ε is set to different values, then the corresponding dynamic responses of these concerned process variables are shown in Figure 4.

Case B: As the power demand signal rises linearly from 50% to 100% in 5 minutes, the error signals in the nuclear power and the average helium temperature cause the power regulator to generate positive speed control action and lift the control rod to reduce this error. The computed responses of reactor process variables corresponding to control action Equation (79) are illustrated in Figures 5 and 6.

Figure 4. Dynamic responses in Case A of (**a**) relative nuclear power; (**b**) average fuel temperature; (**c**) outlet helium temperature and (**d**) control rod speed signal with constant σ and different ε.

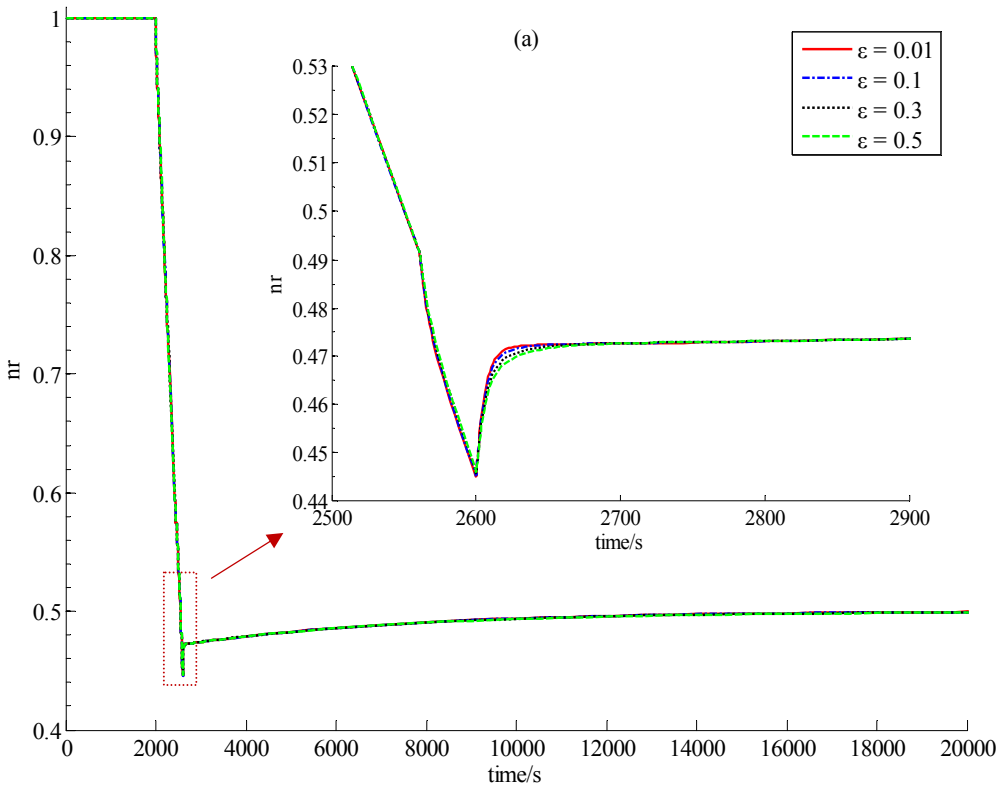

Figure 4. *Cont.*

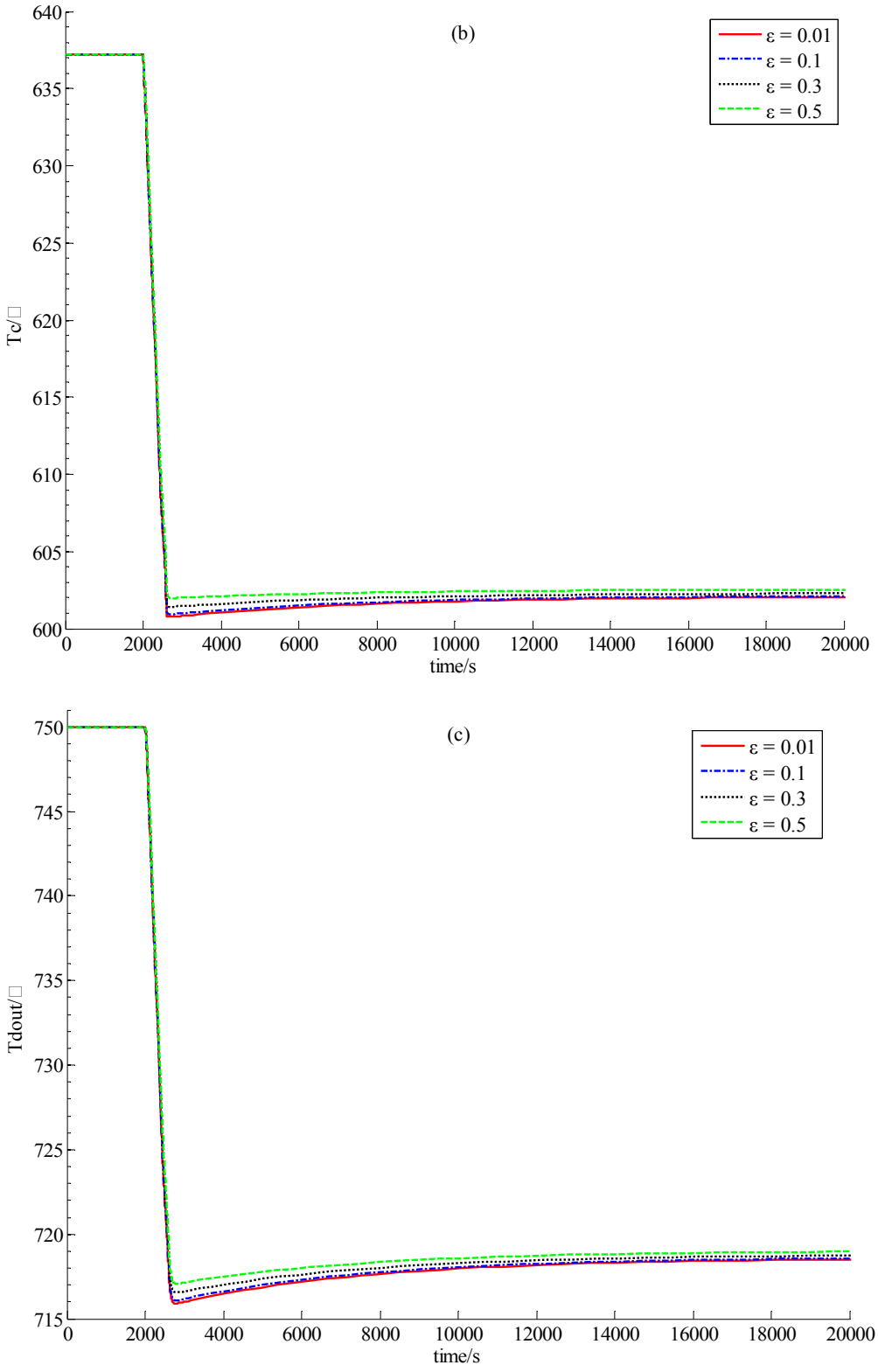

Figure 4. *Cont.*

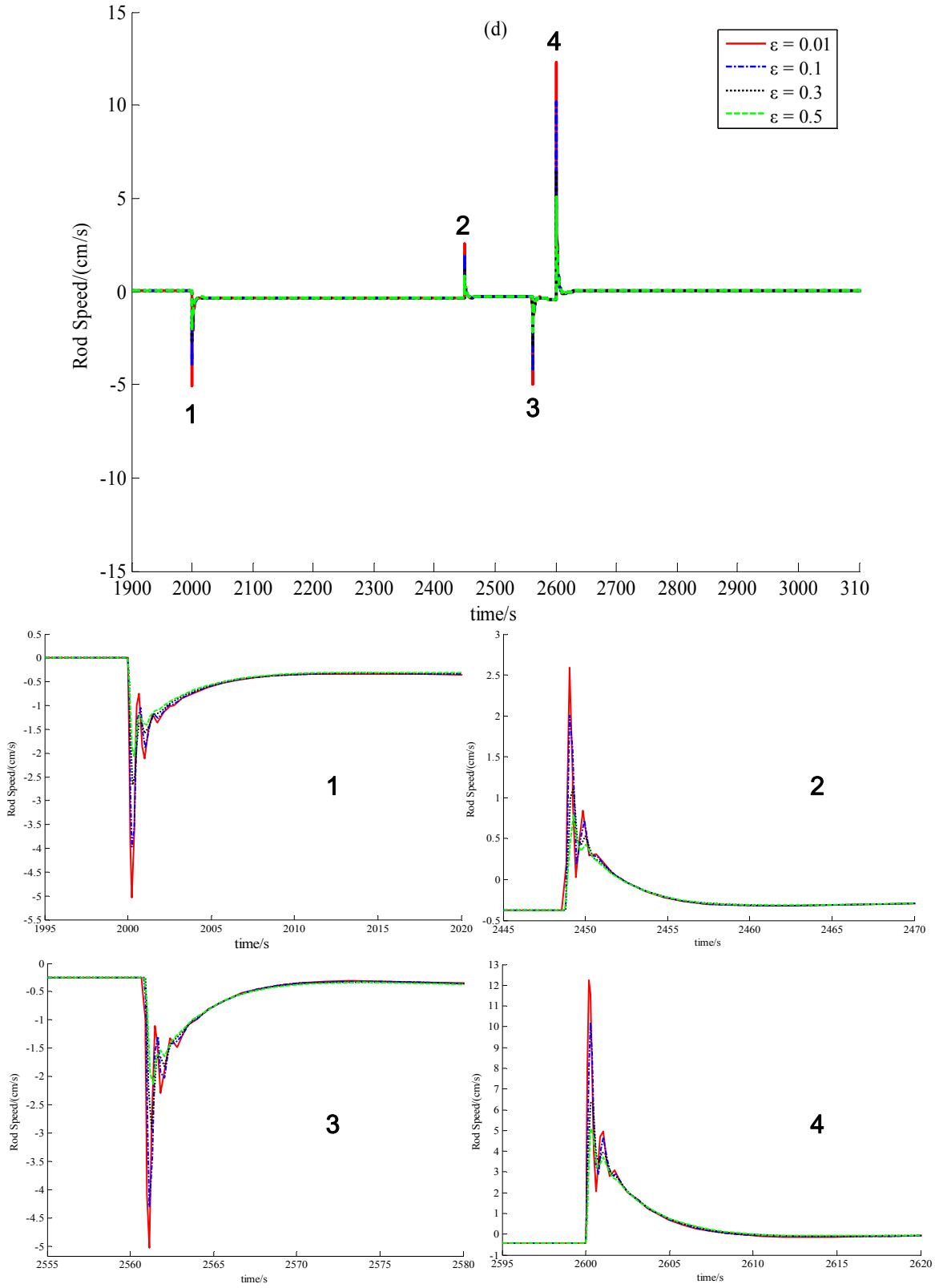

5.3. Discussion

From Figures 3 and 4, the load decrease leads both δn_r and δT_d to be positive and increasing, which drives the power-level controller to give a negative control rod speed signal. Inserting the control rods leads to the decreases of both the nuclear power and fuel temperature. The closed-loop system comes into an equilibrium state if the positive reactivity caused by the decrease of the fuel temperature nearly cancels the negative reactivity caused by the rod insertion. The generation of the control rod speed signal is driven by the variations of both the nuclear power and average coolant temperature obtained from measurement. These two variation signals lead state-observer Equation (78) to give a convergent observation of the state-variations which then cause state-feedback power-level control Equation (63) to generate the speed signal of control rods. Also from Figure 3, we can see that the steady regulation error is smaller if controller parameter σ is larger. Actually, from Equation (56), it is clear that a larger σ can result in a larger L_2 gain from the disturbance to the evaluation signal, which means that the closed-loop system is more robust to both the modeling uncertainty or exterior disturbances. Thus, a smaller steady control error reflects that the closed-loop system has a stronger ability to sustain the disturbances. However, from Proposition 2, to maintain the L_2 disturbance attenuation property of state-feedback law Equation (56), it is necessary to set parameter ε to be a small enough positive scalar. This can be clearly seen from Figure 4 that scalar ε is larger, the L_2 disturbance attenuation performance of the closed-loop is weaker.

Figure 5. Dynamic responses in Case B of (**a**) relative nuclear power; (**b**) average fuel temperature; (**c**) outlet helium temperature and (**d**) control rod speed signal with different σ and constant ε.

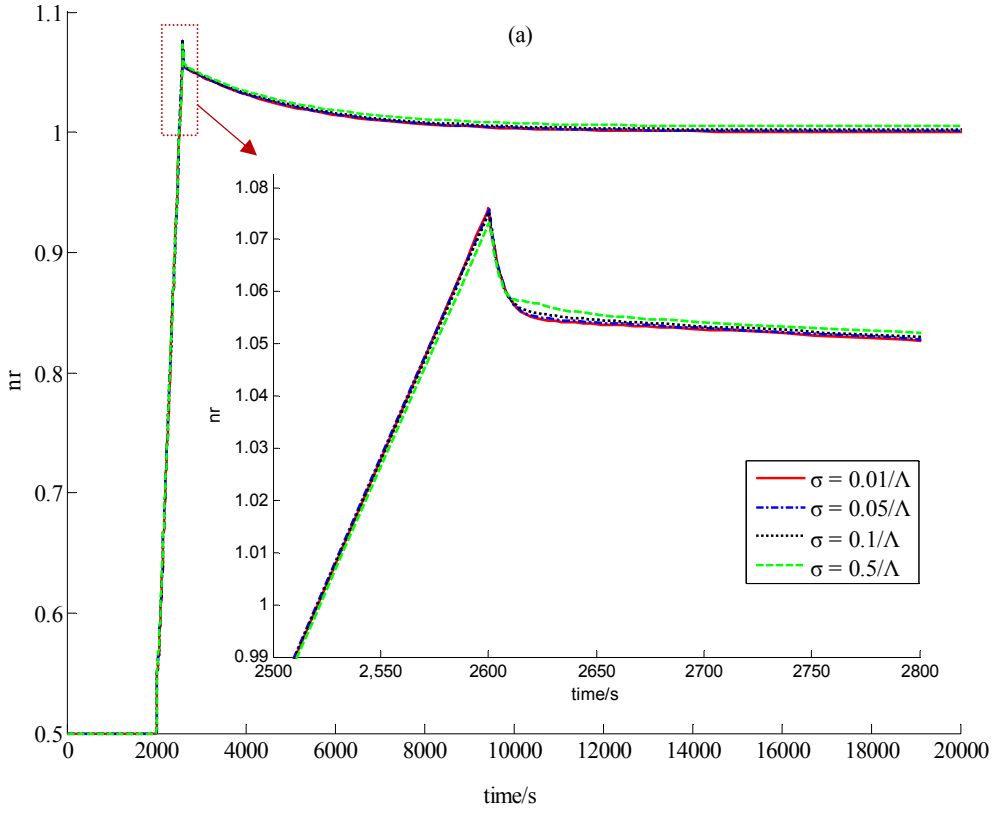

Figure 5. *Cont.*

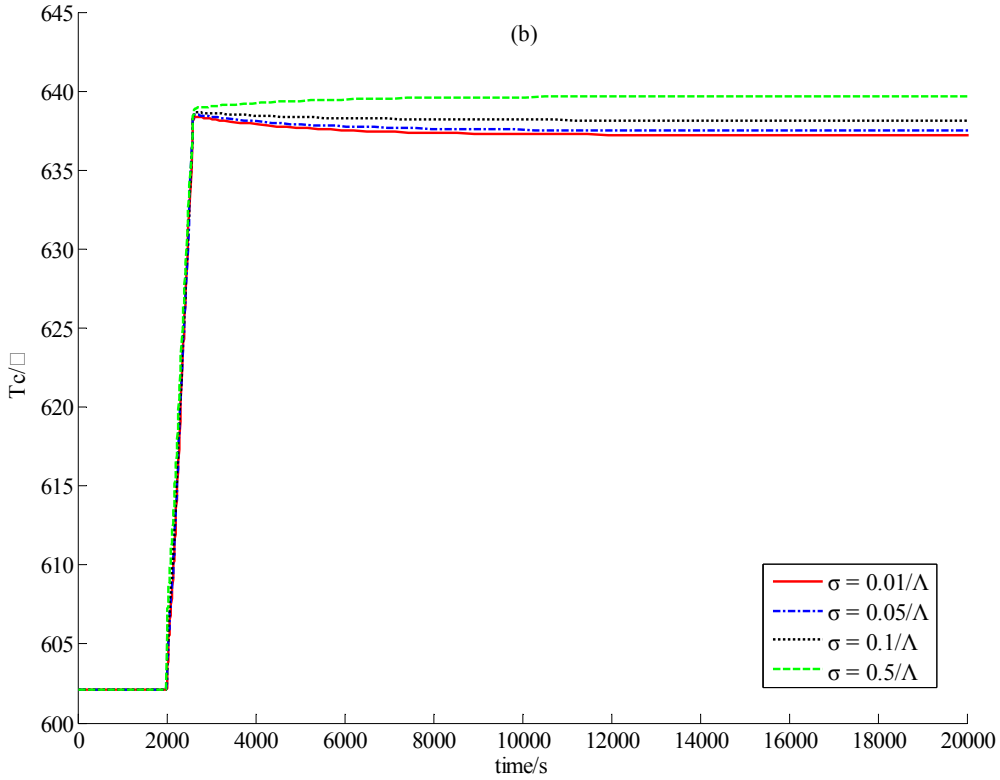

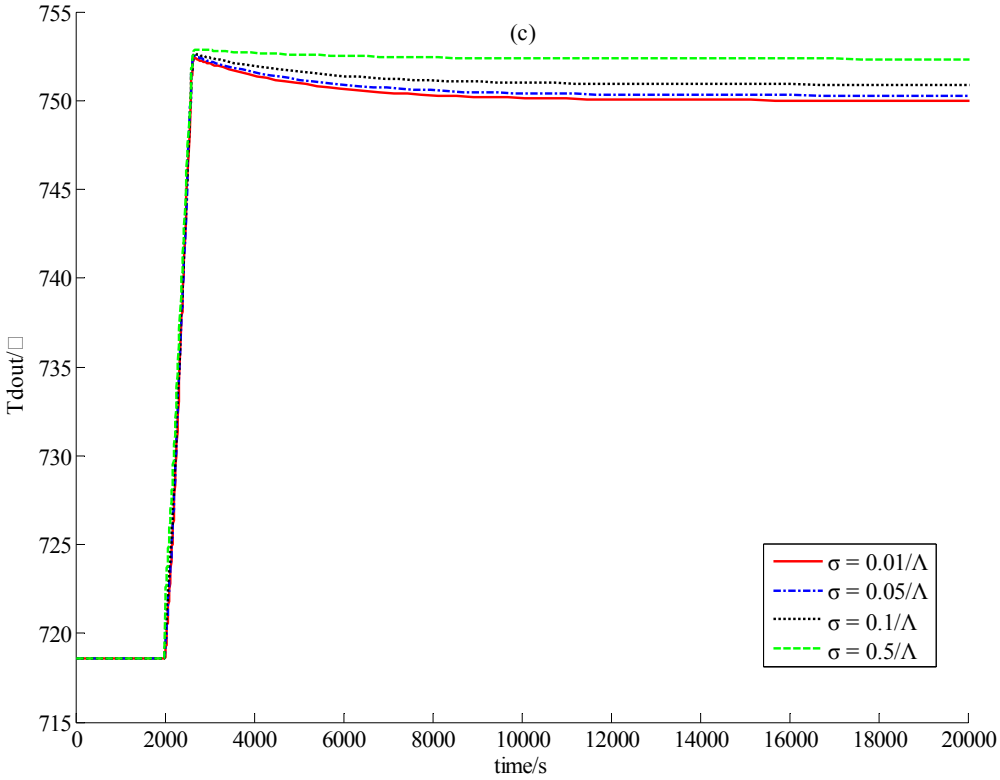

Figure 5. *Cont.*

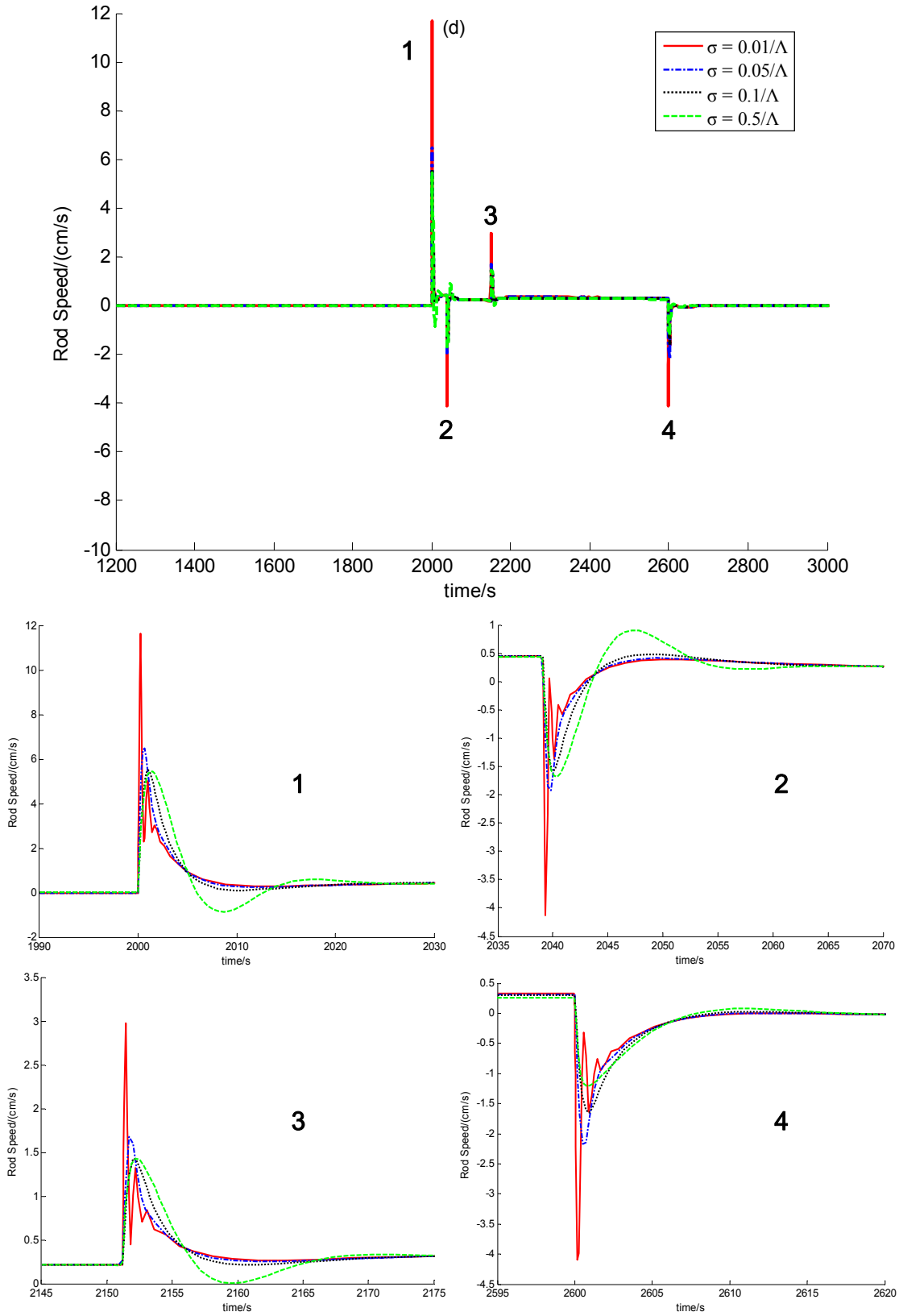

Moreover, from Figures 5 and 6, the load increase causes the decrease of δn_r and δT_d, which results in the generation of a positive speed signal of control rods. The withdrawal of the control rods then causes increases of both the nuclear power and the fuel temperature. Similarly with the case of load drop, the closed-system come to the steady state if the negative reactivity caused by the increase of the fuel temperature nearly cancels the positive reactivity induced by withdrawing the control rods. Moreover, it is clear from Figures 5 and 6 that the control performance is also deeply influenced by the values ε and σ. The reason is the same as that given in the above paragraph.

Finally, from the theoretical analysis and numerical simulation, dynamic output-feedback control strategy Equation (79) is feasible for the power-level regulation of the MHTGRs. The L_2 disturbance attenuation performance of this newly-built control law is guaranteed by choosing the values of both parameters ε and σ to be small enough. With comparison to the power-level controller presented in [29], the transition periods of both the fuel and coolant temperatures caused by the newly-built controller in this paper is much smaller than those corresponding to the controller in [29]. This is just an instance for the fact that dynamic output feedback control is stronger than static output feedback control, and this is also the key improvement of the work in this paper relative to that in [29].

Figure 6. Dynamic responses in Case B of (**a**) relative nuclear power; (**b**) average fuel temperature; (**c**) outlet helium temperature and (**d**) control rod speed signal with constant σ and different ε.

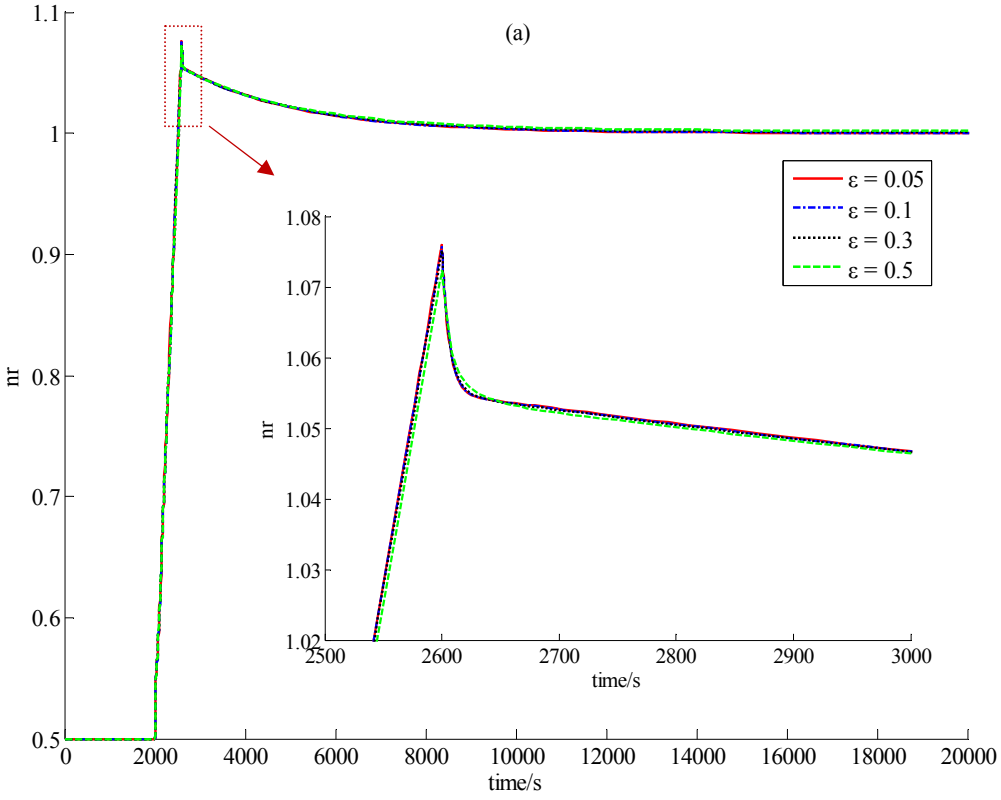

Figure 6. *Cont.*

(b)

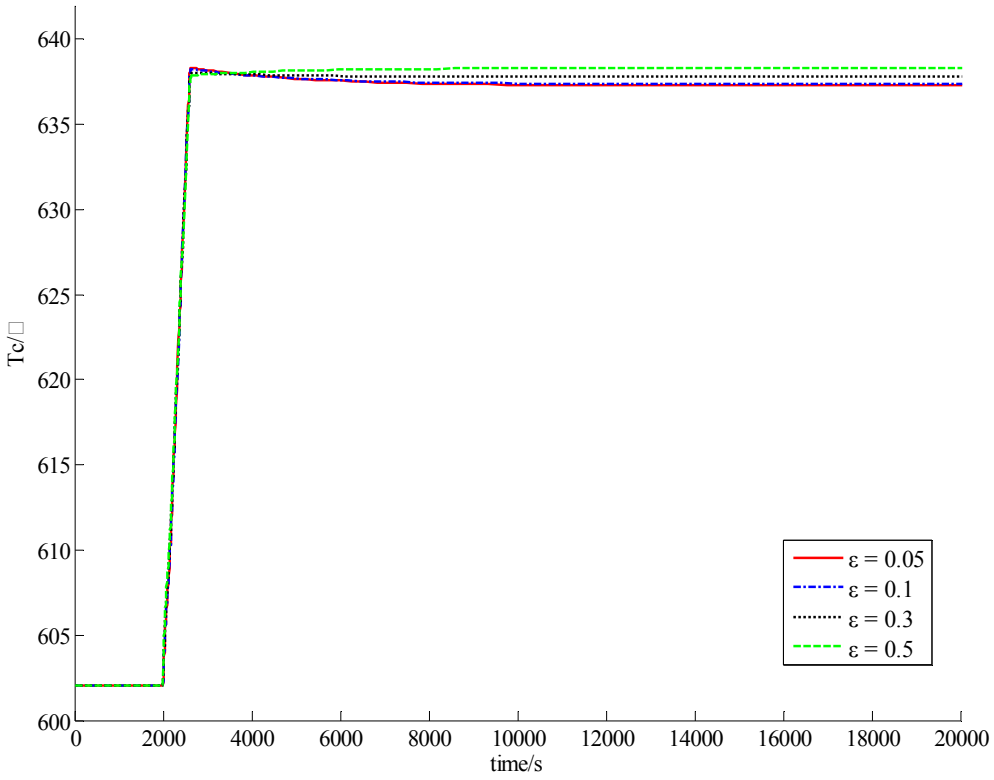

(c)

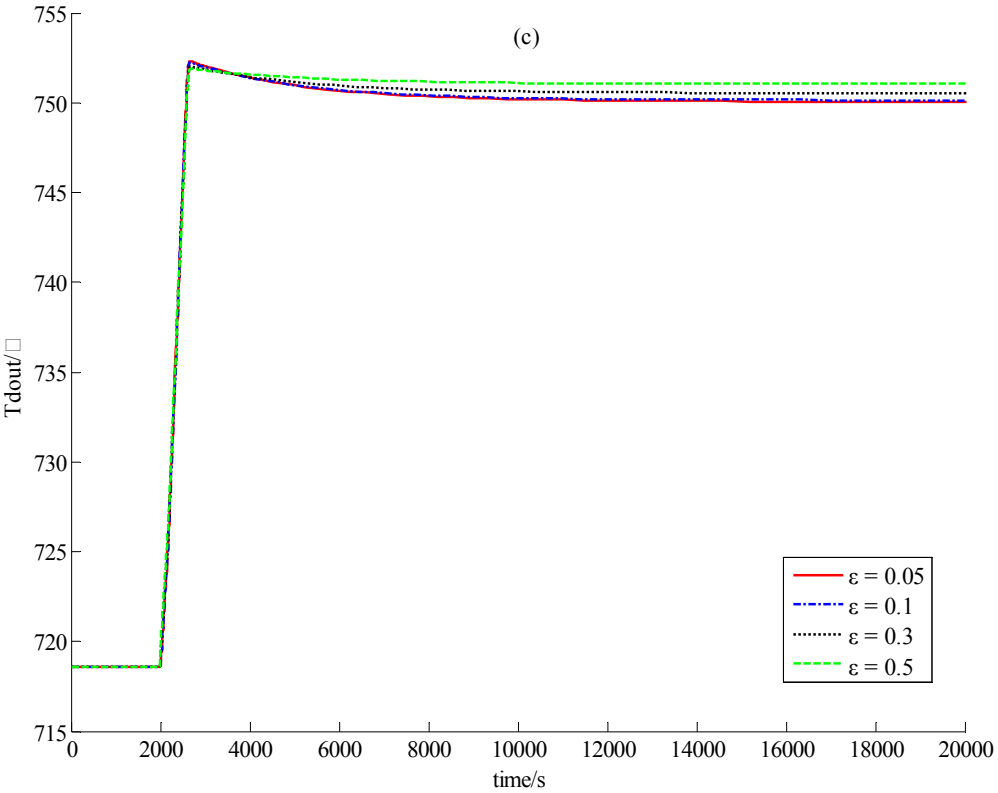

Figure 6. *Cont.*

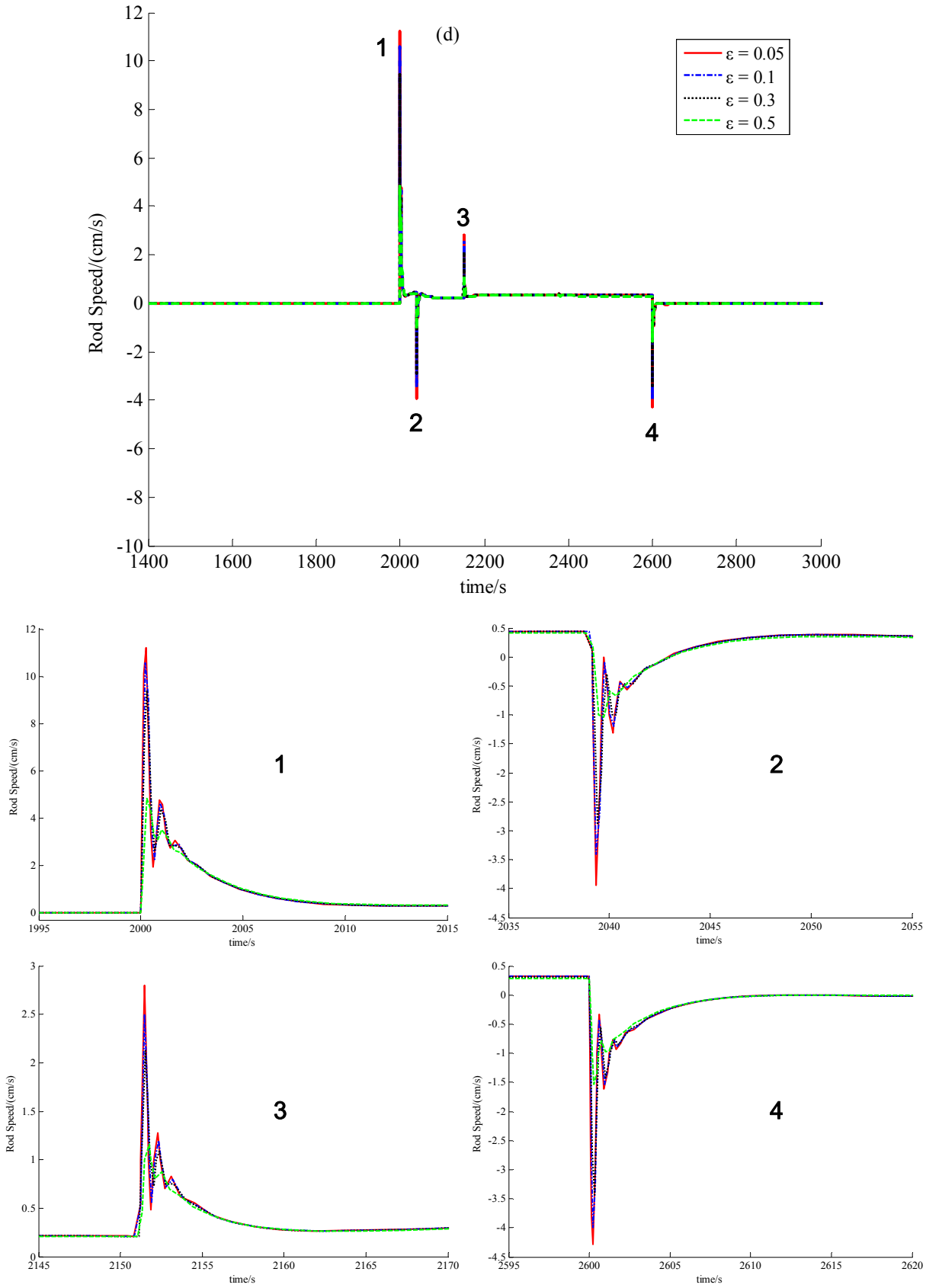

6. Conclusions

Power-level control is a crucial technique for guaranteeing operation stability and efficiency of the MHTGRs. Since the dynamics of the MHTGR are nonlinear and modern state-feedback power-level control has the potential of improving closed-loop stability and control performance, it is necessary to develop a nonlinear power-level control technique for the MHTGR-based nuclear plants. Stimulated by this, a novel nonlinear dynamic output-feedback power-level controller has been given, and the two key techniques of developing this control strategy are respectively the iterative dissipation assignment (IDA) given in Section 3 and the DHGF-based observer design technique given in Section 4. This power-level control strategy can guarantee the L_2 disturbance attenuation performance, and has analytic expressions with clear physical meaning. Moreover, there is a clear relationship between the controller parameters and the regulation performance. Both simulation results and theoretical analysis have shown that the performance of this newly developed power-level controller can be satisfactory high with large enough σ and ε. The results given here have shown the theoretic feasibility of this newly-developed power-level control law. For engineering implementation of this control strategy for the MHTGR such as the reactors of HTR-10 or HTR-PM, the future study lies in verifying the performance of this control strategy on the hardware-in-loop simulation platform proposed in [30].

Acknowledgement

This work is jointly supported by the Natural Science Foundation (Grant No. 61004016) and National S&T Major Project (Grant No.ZX06901) of China. The author would like to thank to the anonymous reviewers for their constructive recommendations. Further, the author would like also to thank Xiaojin Huang for valuable discussions and suggestions.

References

1. Reutler, H.; Lohnert, G.H. The modular high-temperature reactor. *Nucl. Technol.* **1983**, *62*, 22–30.
2. Reutler, H.; Lohnert, G.H. Advantages of going modular in HTRs. *Nucl. Eng. Des.* **1984**, *78*, 129–136.
3. Lohnert, G.H. Technical design features and essential safety-related properties of the HTR-Module. *Nucl. Eng. Des.* **1990**, *121*, 259–275.
4. Wu, Z.; Lin, D.; Zhong, D. The design features of the HTR-10. *Nucl. Eng. Des.* **2002**, *218*, 25–32.
5. Hu, S.; Liang, X.; Wei, L. Commissioning and operation experience and safety experiment on HTR-10. In *Proceedings of 3rd International Topical Meeting on High Temperature Reactor Technology*, Johnanneshurg, South Africa, 1–4 October 2006.
6. Zhang, Z.; Wu, Z.; Wang, D.; Xu, Y.; Sun, Y.; Li, F.; Dong, Y. Current status and technical description of Chinese 2 × 250MW_{th} HTR-PM demonstration plant. *Nucl. Eng. Des.* **2009**, *239*, 1212–1219.
7. Zhang, Z.; Sun, Y. Economic potential of modular reactor nuclear power plants based on the Chinese HTR-PM project. *Nucl. Eng. Des.* **2007**, *237*, 2265–2274.

8. Edwards, R.M.; Lee, K.Y.; Schultz, M.A. State-feedback assisted classical control: An incremental approach to control modernization of existing and future nuclear reactors and power plants. *Nucl. Technol.* **1990**, *92*, 167–185.
9. Ben-Abdennour, A.; Edwards, R.M.; Lee, K.Y. LQR/LTR robust control of nuclear reactors with improved temperature performance. *IEEE Trans. Nucl. Sci.* **1992**, *39*, 2286–2294.
10. Arab-Alibeik, H.; Setayeshi, S. Improved temperature control of a PWR nuclear reactor using LQG/LTR based controller. *IEEE Trans. Nucl. Sci.* **2003**, *50*, 211–218.
11. Shtessel, Y.B. Sliding mode control of the space nuclear reactor system. *IEEE Trans. Aerosp. Electron. Syst.* **1998**, *34*, 579–589.
12. Ku, C.C.; Lee, K.Y.; Edwards, R.M. Improved nuclear reactor temperature control using diagonal recurrent neural networks. *IEEE Trans. Nucl. Sci.* **1992**, *39*, 2298–2308.
13. Na, M.G.; Hwang, I.J.; Lee, Y.J. Design of a fuzzy model predictive power controller for pressurized water reactors. *IEEE Trans. Nucl. Sci.* **2006**, *53*, 1504–1514.
14. Huang, Z.; Edwards, R.M.; Lee, K.Y. Fuzzy-adapted recursive sliding-mode controller design for power plant control. *IEEE Trans. Nucl. Sci.* **2004**, *51*, 1504–1514.
15. Van der Schaft, A.J. *L_2-Gain and Passivity Techniques in Nonlinear Control*; Springer: Berlin, Germany, 1999.
16. Maschke, B.M.; Ortega, R.; van der Schaft, A.J. Energy-based Lyapunov functions for forced Hamiltonian systems with dissipation. *IEEE Trans. Autom. Control* **2000**, *45*, 1498–1502.
17. Ortega, R.; van der Schaft, A.J.; Maschke, B.M.; Escobar, G. Interconnections and damping assignment passivity-based control of port-controlled Hamiltonian systems. *Automatica* **2002**, *38*, 585–596.
18. Ortega, R.; van der Schaft, A.J.; Castaños, F.; Astolfi, A. Control by interconnection and standard passivity-based control of port-Hamiltonian systems. *IEEE Trans. Autom. Control* **2008**, *53*, 2527–2542.
19. Ortega, R.; Spong, M.W.; Gómez-Estern, F.; Blankenstein, G. Stabilization of a class of underactuated mechanical systems via interconnection and damping assignment. *IEEE Trans. Autom. Control* **2002**, *47*, 1218–1233.
20. Fujimoto, K.; Sugie, T. Stabilization of Hamiltonian systems with nonholonomic constraints based on time-varying generalized canonical transformations. *Syst. Control Lett.* **2001**, *44*, 309–319.
21. Liu, Q.J.; Sun, Y.Z.; Shen, T.L.; Song, Y.H. Adaptive nonlinear coordinated excitation and STATCOM controller based on Hamiltonian structure for multimachine power-system stability enhancement. *IET Proc. Control Theory Appl.* **2003**, *50*, 285–294.
22. Wang, Y.; Cheng, D.; Li, C.; Ge, Y. Dissipative Hamiltonian realization and energy-based L_2-disturbance attenuation control of multi-machine power systems. *IEEE Trans. Autom. Control* **2003**, *48*, 1428–1433.
23. Galaz, M.; Ortega, R.; Bazanella, A.S.; Stankovic, A.M. An energy-shaping approach to the design of excitation control of synchronous generators. *Automatica* **2003**, *39*, 111–119.
24. Dong, Z.; Feng, J.; Huang, X.; Zhang L. Dissipation-based high gain filter for monitoring nuclear reactors. *IEEE Trans. Nucl. Sci.* **2010**, *57*, 328–339.
25. Dong, Z.; Huang, X.; Zhang, L. Output feedback power-level control of nuclear reactors based on a dissipative high gain filter. *Nucl. Eng. Des.* **2011**, *241*, 4783–4793.

26. Li, H.; Huang, X.; Zhang, L. A simplified mathematical dynamic model of the HTR-10 high temperature gas-cooled reactor with control system design purpose. *Ann. Nucl. Energy* **2008**, *35*, 1642–1651.
27. Dong, Z.; Huang, X.; Zhang, L. A nodal dynamic model for control system design and simulation of an MHTGR core. *Nucl. Eng. Des.* **2010**, *240*, 1251–1261.
28. Li, H.; Huang, X.; Zhang, L. A lumped parameter dynamic model of the helical coiled once-through steam generator with movable boundaries. *Nucl. Eng. Des.* **2008**, *238*, 1657–1663.
29. Dong, Z. Output feedback dissipation control for the power-level of modular high-temperature gas-cooled reactors. *Energies* **2011**, *4*, 1858–1879.
30. Dong, Z.; Huang, X. Real-time simulation platform for the design and verification of the operation strategy of the HTR-PM. In *Proceedings of the 19th International Conference on Nuclear Engineering*, Chiba, Japan, 16–19 May 2011.